Eocene-Oligocene extinction and paleoclimatic change near Eugene, Oregon

Gregory J. Retallack†
William N. Orr
Department of Geological Sciences, University of Oregon, Eugene, Oregon 97403, USA

Donald R. Prothero
Department of Geology, Occidental College, Los Angeles, California 90041, USA

Robert A. Duncan
College of Oceanic and Atmospheric Sciences, Oregon State University, Corvallis, Oregon 97331, USA

Paul R. Kester
Department of Earth and Space Sciences, University of Washington, Seattle, Washington 98195, USA

Clifford P. Ambers
Department of Environmental Studies, Sweet Briar College, Sweet Briar, Virginia 24595, USA

ABSTRACT

Thick ash-flow tuffs provide marker beds through fossiliferous Eocene and Oligocene marine and non-marine sedimentary rocks near Eugene, Oregon. New mapping, radiometric dating, and paleomagnetic stratigraphy of these tuffs and rocks now allow dating of local fossil floras. The Comstock, Goshen, Rujada, and Willamette floras have been widely used as evidence for Eocene-Oligocene climatic cooling and drying. Eocene leaves from Comstock and Hobart Butte included such thermophilic taxa as *Liquidambar*. The early Oligocene Goshen flora lacked *Liquidambar* but retained many thermophilic species with large leaves that have entire margins and acuminate apices (drip tips). In contrast, fossil leaves from later Oligocene Rujada and Willamette floras are small and serrate, and most lack drip tips. Marine faunas also indicate climatic cooling and local disappearance of thermophilic molluscs such as *Anadara*, *Ficus*, and *Conus*. Our dating and compilation of plant and molluscan fossil occurrences indicate a steady rise in species diversity from 46 Ma to maximal diversity of thermophilic taxa at 35–34 Ma, then extinctions of 60% of plant species after 33.4 Ma and 32% of marine invertebrates after 33.2 Ma, both significantly postdating the Eocene-Oligocene boundary at 33.7 Ma. Plant diversity rebounds during the early Oligocene, but marine invertebrates continue to decline into the Oligocene in part due to the retreat of fully marine environments from the Eugene area. Neither these data, nor evidence from coeval fossil plants and soils in central Oregon, support the notion of a "Terminal Eocene Event," nor any other single, abrupt paleoclimatic shift or extinction. The Eocene-Oligocene biotic and climatic transition was drawn out over some 6 m.y. Abrupt forcings such as meteorite impacts or volcanic eruptions are less likely explanations for cooling and diversity decline than long-term processes such as mountain building, changing ocean currents, or reorganization of the carbon cycle by coevolution of grasses and grazers.

Keywords: Eocene-Oligocene, Eugene, Oregon, fossil floras, ash-flow tuffs.

INTRODUCTION

The Eocene-Oligocene transition has long been regarded as a turning point between Eocene greenhouse paleoclimate and a near-modern climatic regime (Chaney, 1948; Prothero, 1994a). It is close in time to one of the most striking inflections in the Cenozoic record of the carbon and oxygen isotopic composition of deep-sea foraminifera (Zachos et al., 2001). One explanation for this profound paleoclimatic shift has been the continental drift of Australia and South America away from Antarctica, which encouraged ice sheet growth by thermal isolation due to initiation of the circum-Antarctic current (Exon et al., 2002). Another explanation is cooling by drawdown of atmospheric carbon dioxide due to silicate weathering stimulated by mountain building (Raymo and Ruddiman, 1992). Yet another explanation is the spread of grasses and grazers, which create more rapidly weathered soils of greater carbon storage capacity, sediments of higher carbon content, and ecosystems with higher albedo and lower transpiration than preexisting woodlands (Retallack, 2001a). There were also late Eocene meteorite or comet impacts, which are indicated by iridium anomalies (Montanari et al., 1993); shocked quartz (Clymer et al., 1996; Langenhorst and Clymer, 1996); ^{3}He anomalies (Farley et al., 1998); tektite-strewn fields (Glass and Zwart, 1979; Glass et al., 1986; Glass, 1990); and the Chesapeake, Toms Canyon, and Popigai impact craters (Bottomly et al., 1993; Poag et al., 1994, 2003; Poag and Aubry, 1995). Also close to the Eocene-Oligocene boundary were extinctions of marine foraminifera (Berggren et al., 1995), marine molluscs (Squires, 2003; Hickman, 2003), echinoids (Oyen and Portell, 2001; Burns and Mooi, 2003), land snails (Evanoff et al., 1992), land plants (Wolfe, 1992; Ridgway et al., 1995), reptiles, amphibians (Hutchison, 1992), and mammals (Prothero, 1994b; Janis, 1997).

The relative timing of extinction and paleoclimatic change on land and in the sea is addressed here with new mapping and radiometric and paleomagnetic dating of sedimentary and volcanic rocks near Eugene, Oregon. Local Goshen and Willamette floras figure prominently in paleoclimatic reconstructions (Wolfe, 1981a, 1994, 1995). These fossil floras are separated by only 2 km along Interstate 5, and both floras are south along strike from shallow marine rocks (Figs.1–3; Rathbun, 1926; Steere, 1958;

†E-mail: gregr@darkwing.uoregon.edu.

GSA Bulletin; July/August 2004; v. 116; no. 7/8; p. 817–839; doi: 10.1130/B25281.1; 19 figures; 4 tables; Data Repository item 2004103.

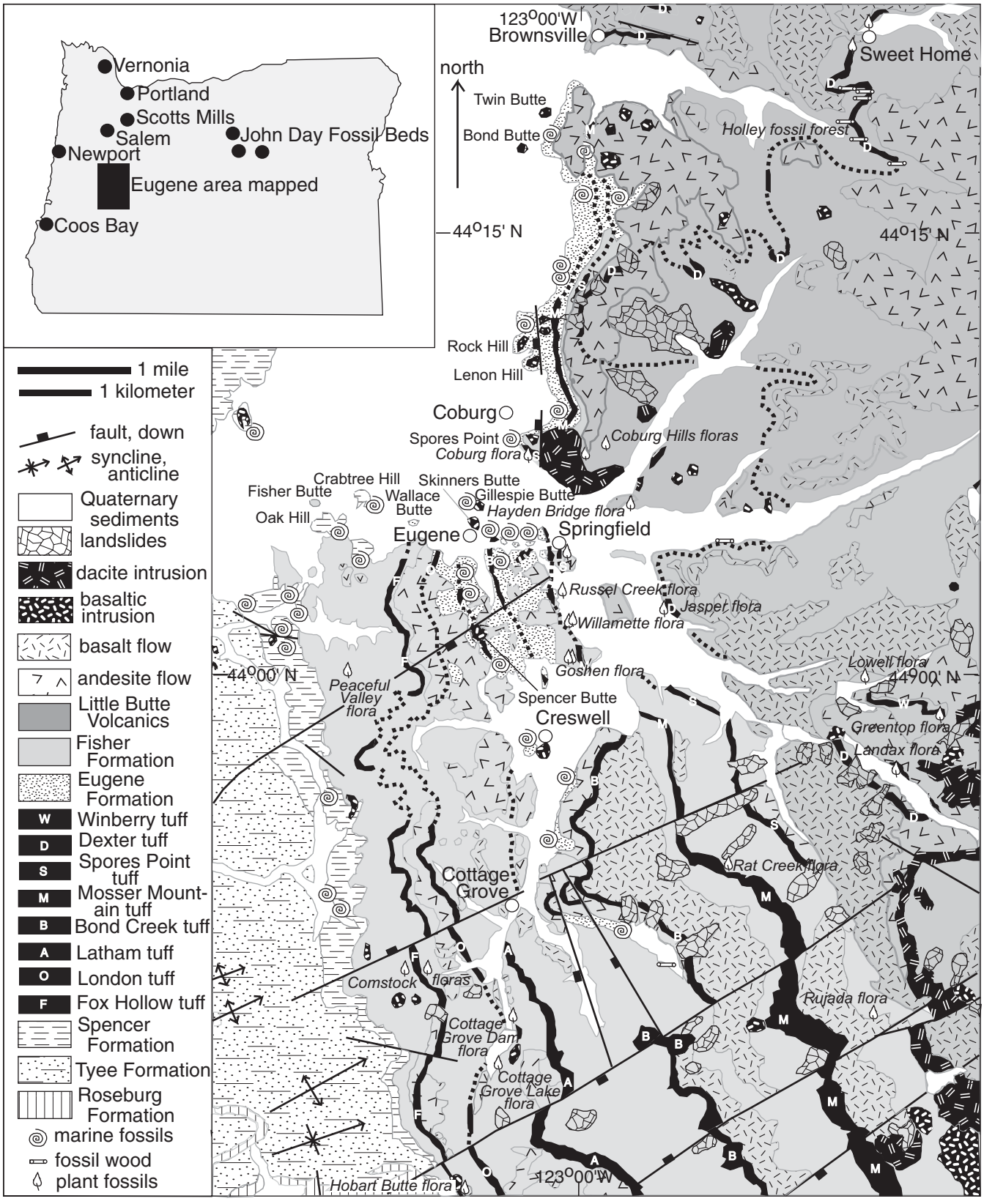

Figure 1. Geological map emphasizing tephrostratigraphy of Eocene and Oligocene rocks near Eugene, Oregon (mapping by Retallack, with data from Schenk, 1923; Lewis, 1951; Hausen, 1951; Ashwill, 1951; Bales, 1951; Vokes et al., 1951; MacPherson, 1953; Bristow, 1959; Hauck, 1962; Anderson, 1963; Peck et al., 1964; Maddox, 1965; Baldwin, 1981; Sherrod and Smith, 2000).

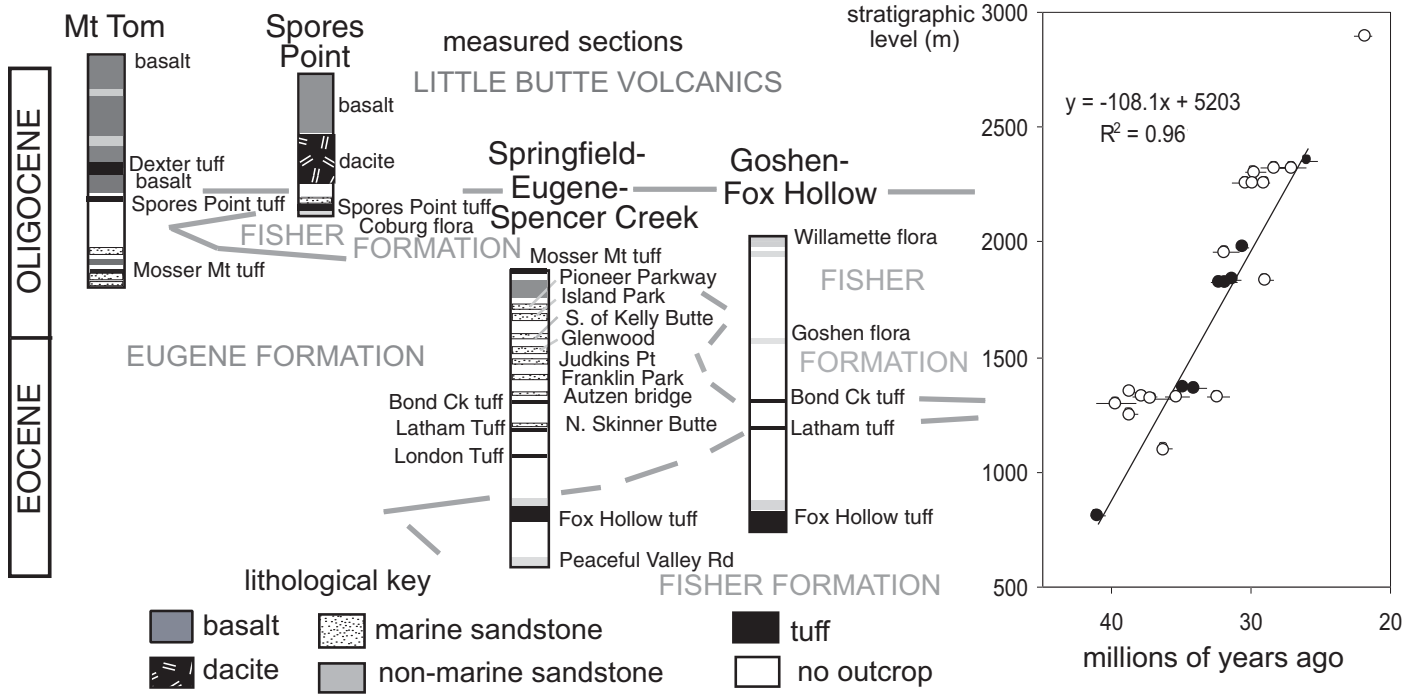

Figure 2. Long measured sections of Eocene and Oligocene rocks near Eugene, Oregon, and their age interpolated from new $^{40}Ar/^{39}Ar$ age determinations (closed symbols). All sections measured by Retallack. Also shown are old K-Ar age determinations (open symbols).

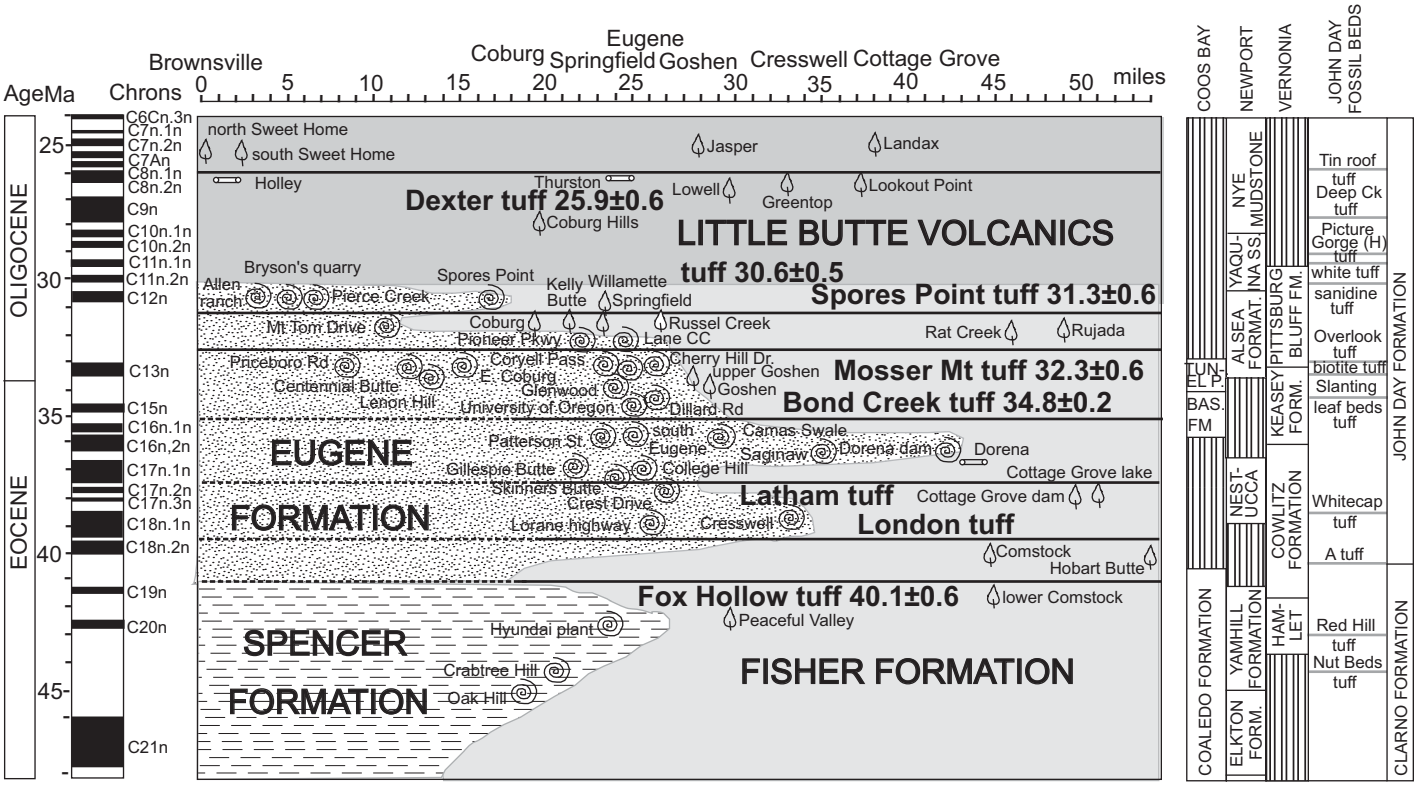

Figure 3. Distribution of fossil sites in north-south transect from Brownsville, through Eugene, to south of Cottage Grove. Correlations with other areas of Oregon are from Bestland et al. (1999), Retallack et al. (2000), Prothero (2001), Prothero and Donohoo (2001a, 2001b), Prothero and Hankins (2000, 2001), and Prothero et al. (2001a, 2001b).

Hickman, 1969). The Goshen flora has large leaves of tropical floristic and climatic affinities that are like those of underlying Eocene floras and unlike those of overlying temperate floras such as the Oligocene Willamette flora. Using leaf physiognomic data, Wolfe (1978) proposed a decline of 12–13 °C in mean annual temperature and an increase in mean annual range of temperature of ~10 °C at what he called the "Terminal Eocene Event," which occurred over less than 1 m.y. across the Eocene-Oligocene boundary. On the other hand, Axelrod (1992) interprets the same floras and their relationships as a climatic cooling drawn out over some 6 m.y. Estimating the rapidity of this climate change has been difficult, because radiometric and paleomagnetic calibration of the Eocene-Oligocene boundary has been through an unusually turbulent period of revision, bouncing around between 38 and 32 Ma (Swisher and Prothero, 1990). New $^{40}Ar/^{39}Ar$ radiometric dates and establishment of a global stratotype section at Massignano, Italy, have now settled the boundary at 33.7 Ma (Berggren et al., 1995). This has had surprising ramifications for local biostratigraphic schemes. The Eocene-Oligocene boundary is now between the Chadronian and Orellan North American Land Mammal "Ages" (Prothero and Whittlesey, 1998), between the Kummerian and Angoonian floral stages (Wolfe, 1981a), within the late Refugian local foraminiferal stage, and within the late Galvinian local molluscan stage (Prothero, 2001; Armentrout, 1981; Squires, 2003; Nesbitt, 2003). Interfingering Galvinian-Refugian marine and Kummerian–Angoonian non-marine sedimentary rocks near Eugene offer the prospect of obtaining a coherent narrative of both marine and terrestrial biotic change at the end of the Eocene.

A NEW TEPHROSTRATIGRAPHY

A series of marker tuff beds proved the key to new mapping and section measuring of complex marine and non-marine sediments and lavas near Eugene (Figs. 1–3). The marker tuffs are thick and exposed on strike ridges, which can be mapped in this forested and built landscape of limited rock exposures (Fig. 1). Individual tuffs vary considerably in degree of welding and proportion of crystals, shards, and rock fragments, both in vertical section and along strike (Hausen, 1951), but mineral content and crystal form visible in thin section were used to support mapping (Table 1). The marker tuffs are all more or less rhyodacitic in composition (Fig. 4; Murray, 1994). They were ash-flow tuffs, presumably formed from large caldera eruptions and Plinian column collapse, as proposed for Eocene and Oligocence ash-flow tuffs of eastern Oregon (Fisher, 1966).

The late Eocene Bond Creek tuff (35 Ma) has been mapped along strike for 200 km from Eugene south to Ashland (Smith et al., 1980; Hladky et al., 1992; Torley and Hladky, 1999). It is 25 m thick at the Masonic Cemetery in south Eugene but 210 m thick closer to its source near Dorena Dam (Hausen, 1951) and 160 m thick near Medford (Murray, 1994). The early Oligocene (31 Ma) Mosser Mountain tuff is 230 m thick in its type area near Medford (Murray, 1994) but only 10 m thick at Buck Mountain, north of Coburg. The late Oligocene Dexter tuff (26 Ma) is 183 m thick in its type area south of Dexter but only 14 m thick near Brownsville (Anderson, 1963) and Sweet Home (Richardson, 1950). About 4 m of the early Miocene Winberry tuff (22 Ma) within the area mapped was presumably derived from a caldera to the east and south (Ashwill, 1951; Woller and Priest, 1982; Millhollen, 1991).

Some of these tuffs may also extend into eastern Oregon, where ash-flow tuffs have been used as stratigraphic markers (Robinson et al., 1984). The basal John Day A tuff of central Oregon is of comparable age to the Fox Hollow tuff; the Whitecap tuff is comparable to the Latham tuff; the Overlook tuff is comparable to the Mosser Mountain tuff; and the Tin Roof tuff is comparable to the Dexter tuff (Fremd et al., 1994; Bestland et al., 1999; Retallack et al., 2000). The Colestin Formation of southwestern Oregon and northwestern California may include equivalents of the Fox Hollow, Bond Creek, and Dexter tuffs (Chocolate Falls tuff, biotite tuff of Tcl, and crystal tuff of Tct, respectively, of Bestland, 1987). Even without such correlations, these were large eruptions of wide geographic distribution.

These thick tuffs are especially useful stratigraphic markers because sedimentary and volcanic rocks near Eugene have complex geometry (Smith, 1938; Vokes et al., 1951), and because fossil faunas include beach, estuarine, and intertidal assemblages lacking fossils that are biostratigraphically similar to open marine faunas of Washington and California (Hickman, 1969, 2003; McDougall, 1980; Nesbitt, 2003). These marker tuffs confirm that the non-marine Fisher Formation is laterally equivalent to the marine

TABLE 1. TEPHROSTRATIGRAPHY NEAR EUGENE, OREGON

Tuff	Type section	Coordinates	Thickness (m)	Age (Ma)	Quartz	Plagioclase	Lithic	Other minerals
Winberry	Southern slopes of Winberry Mountain	SE¼NW¼SE¼ S20 T19S R2E	>4.0	21.6	Rare	Zoned	Shards	Ferriaugite, ferrisilite
Dexter	Highway 58 roadcuts 3 mi E Dexter, Lane Co.	NW¼NE¼NW¼ S24 T19S R1W	183	25.9	Small rounded	Large zoned	Volcanic	Biotite, pyroxene
Spores Point	McKenzie River bank, Spores Point, Lane Co.	SE¼SE¼NW¼ S10 T17S R3W	6	31.3	Small, euhedral	Small, twinned	Common pumice	—
Mosser Mountain	6 mi. S Shady grove, Jackson Co.	SW¼SE¼NW¼ S15 T35S R1W	370	31.2	Embayed, rounded	Large zoned	Volcanic	—
Bond Creek	5 mi S Glide, Douglas Co.	NE¼NE¼NE¼ S11 T27S R3W	160	34.9	Euhedral, embayed	Large zoned	Pumice	Biotite
Latham	Latham exit from Interstate 5 Lane Co.	SE¼SE¼NW¼ S4 T21S R3W	8	36?	Rare	Large zoned	Volcanic	Biotite
London	Interstate 5 roadcut 9 mi. N London, Lane Co.	NE¼SE¼SW¼ S11 T21S R4W	9	38?	Rare	Euhedral unzoned twinned	Volcanic	—
Fox Hollow	Lorane highway 0.5 mi W Spencer Grange, Lane Co.	SE¼SE¼NW¼ S22 T18S R4W	74	40.1	Euhedral, embayed	Zoned twinned	Pumice, volcanic	Augite, magnetite

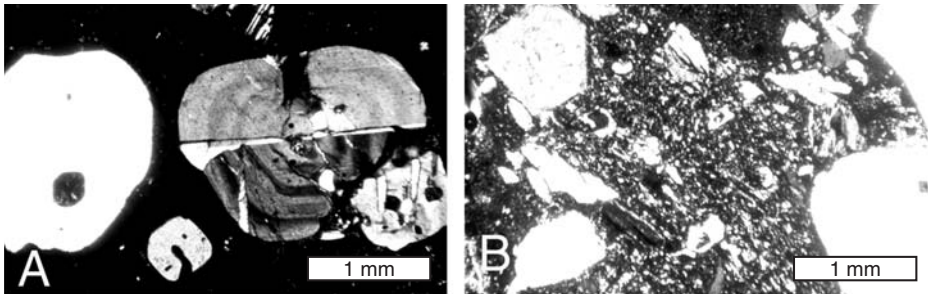

Figure 4. Photomicrographs of selected tuff marker beds, including Mosser Mountain tuff near Buck Mountain (A) and Bond Creek tuff on Willamette River north of Patterson Street (B). Zoned plagioclase is abundant and quartz is somewhat resorbed in Mosser Mountain tuff, whereas Bond Creek tuff has idiomorphic quartz and zoned plagioclase as well as biotite and rock fragments. Scales are both 1 mm.

Spencer and Eugene Formations (Vokes and Snavely, 1948; Vokes et al., 1951; Graven, 1990). The Eugene and Fisher Formations are overlain by the Little Butte Volcanics. The lower boundary of the Little Butte Volcanics that worked best for the current mapping (Fig. 1) was below dacites and basalts, which fill paleovalleys of an erosional disconformity along the base of the steep western face of the Coburg Hills (Lewis, 1951). The Little Butte Volcanics are largely andesite and dacite flows but include some interflow sediment and the Dexter tuff and overlie tuffaceous sediments above the Spores Point tuff. Basalt and dacite flows and intrusions are scattered through the Fisher Formation as well, but in the Little Butte Volcanics they dominate the sequence. The Fox Hollow tuff forms a mappable base to the Eugene Formation. Marine fossils collected in 1996 from excavations for the Hyundai factory southeast of Oak Hill include molluscs such as *Turritella uvasana,* which is characteristic of Eocene tropical Coaledo-Cowlitz faunas rather than those of the Eugene Formation between Eugene and Springfield (Schenk, 1923; Hickman, 2003). Previous fossil collections from nearby Oak and Crabtree Hills included only long-ranging nearshore molluscs (Hickman, 1969).

The tuffs are also useful as isochronous planes cutting across sedimentary facies to reveal lateral paleoenvironmental variation. The Bond Creek tuff is found within both the non-marine Fisher Formation to the south and the marine Eugene Formation to the north. Within the framework of marker tuffs, marine transgression and regression north-south from Brownsville to Cottage Grove can be measured within time slices defined by marker tuffs (Fig. 3). This paleoslope was also revealed by paleocurrents of trough cross-bedding within fluvial paleochannels in the Fisher Formation (Fig. 5). All four ancient streams flowed more or less northerly from the Klamath Mountains and southwestern Cascades into an Eocene-Oligocene marine embayment in the current area of the Willamette Valley.

Coastal facies along this migrating shoreline include sandstones that are relatively rich in quartz for these predominantly volcaniclastic litharenites (Schenk, 1923; Mears, 1989; Lowry, 1947), perhaps due to eolian and surf reworking. Supratidal facies can be inferred from halite crystal pseudomorphs in tuffs of Bryson's quarry 4 mi southwest of Brownsville (Vokes and Snavly, 1948) and within fossil wood of the Sweet Home fossil forests (Staples, 1950). Near-shore, shallow-marine environments are indicated by sedimentary structures such as hummocky cross-bedding, shallow water trace fossils such as *Planolites* and *Thalassinoides* (Figs. 6–8) and common glauconite and phosphate nodules (Mears, 1989). Sandstones and siltstones with siderite nodules containing fossil molluscs and crabs (Rathbun, 1926) and siltstones with clams (especially *Solena eugenensis* and *Macoma vancouverensis)* in growth position were probably also very shallow subtidal to low intertidal. Fossil plants are common in these shallow marine rocks, and some plant fragments are permineralized by calcite. These include mainly fossil twigs and logs, which are often bored by shipworms (*Martesites* sp.; Hickman, 1969), but also unexpected items such as permineralized fruit-stones of icacina vine (*Palaeophytocrene foveolata*) and conifer cones.

Among non-marine facies are lacustrine beds of varved shales that are especially well exposed at the Willamette and Rujada flora localities (Myers et al., 2002). Many of the sandstones and conglomerates of the Fisher and Little Butte Volcanics show fluvial fining-upward sequences from conglomerates to trough cross-bedded sandstone, rippled marked sandstone, and paleosols. Most of the paleosols are very weakly developed (Entisols). Well-developed paleosols with smectite clays (Gleyed Inceptisols) are best seen in road cuts exposing claystones overlying the Goshen flora and the Willamette flora. Strongly developed red paleosols were seen capping the Fox Hollow tuff (40 Ma) at several places along strike: Wallace Butte, along Fox Hollow Road, west of Cottage Grove Lake, and near Hobart Butte. Other strongly developed red paleosols cap the Bond Creek tuff (35 Ma) in the hills east of Saginaw and the Dexter tuff (26 Ma) at Cascadia State Park near Sweet Home. The Wallace Butte and Saginaw red paleosols are thick (more than 5 m) and kaolinitic (Fig. 9) with very high alumina content (35.70 and 29.55 wt%, respectively) and alkali and alkaline earth oxides cumulatively less than 2 wt% (Wilson and Treasher, 1938; E. Eddings, personal commun., 1997). Comparable red beds and paleosols were found at many levels within subsurface Fisher Formation drilled 4 km northeast of Cresswell by Guarantee Oil in 1927. Eocene lateritic paleosols of comparable geological ages are also known in central Oregon, where they have been identified as Oxisols and Ultisols (Bestland et al., 1996; Retallack et al., 2000).

RADIOMETRIC DATING

Numerous K-Ar dates have been reported for tuff, basalt, and andesite flows around Eugene (Lux, 1981; Feibelkorn et al., 1982), but after correction to the same constants (Dalrymple, 1979), indications of inaccuracy include errors from large proportions of atmospheric argon and violations of stratigraphic superposition

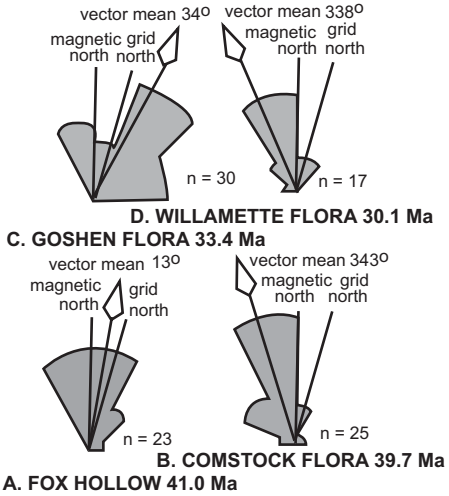

Figure 5. Paleocurrents measured (by Retallack) from orientation of trough cross beds in fluvial paleochannels of Fisher Formation (see Figure 6 for measured sections).

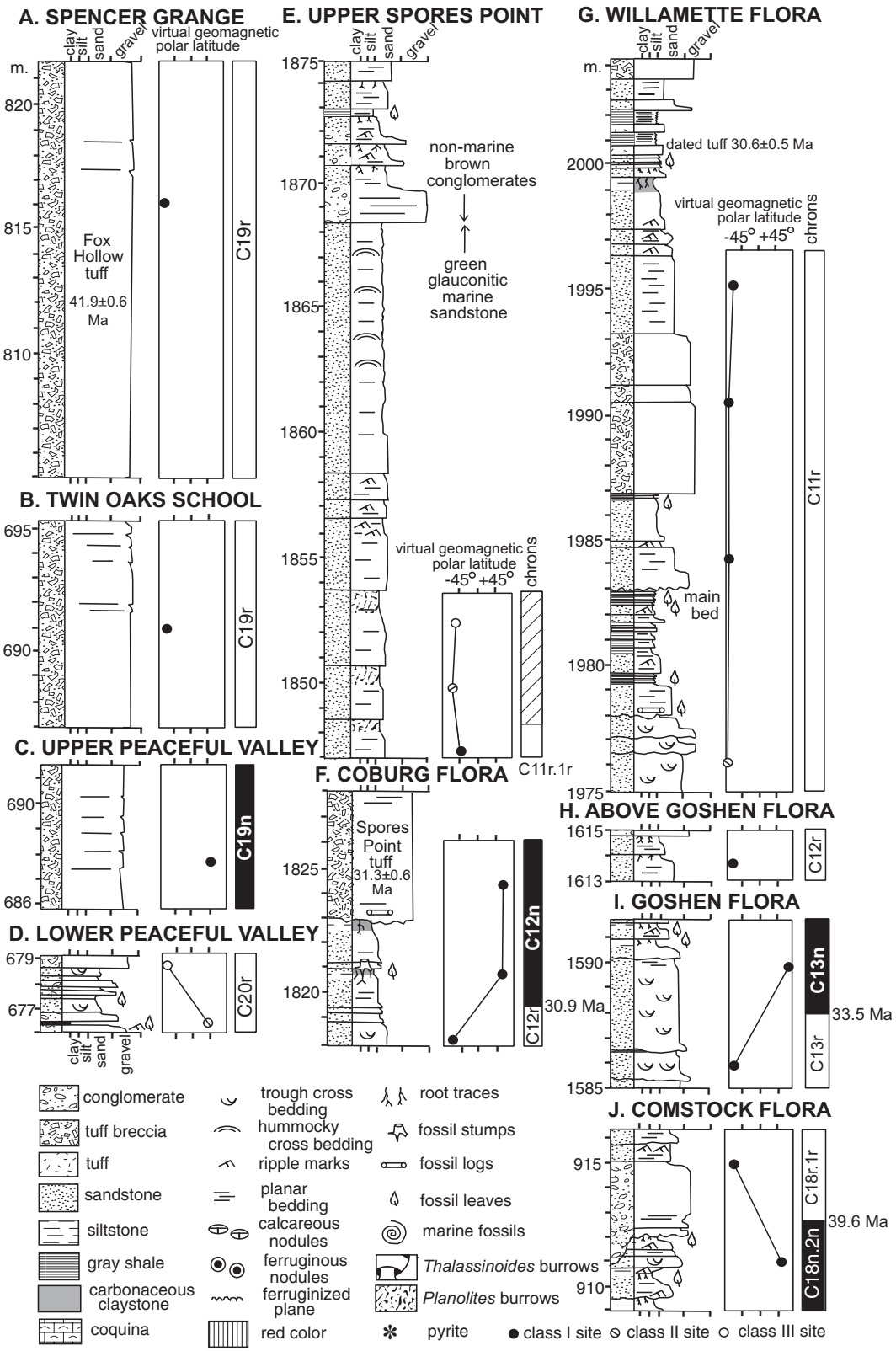

Figure 6. Sedimentological and paleomagnetic observations of non-marine Fisher Formation at selected fossil plant localities near Eugene, Oregon. Meter levels are from composite stratigraphic sections of Figure 2. All sections measured and logged by Retallack, with paleomagnetic data by Prothero. Solid circles indicate class I paleomagnetic sites where all three directions are significantly clustered and distinct from random. Slashed circles are class II sites missing a sample, so that site statistics could not be calculated. Open circles are class III sites for which one vector was divergent, but the other two showed clear polarity.

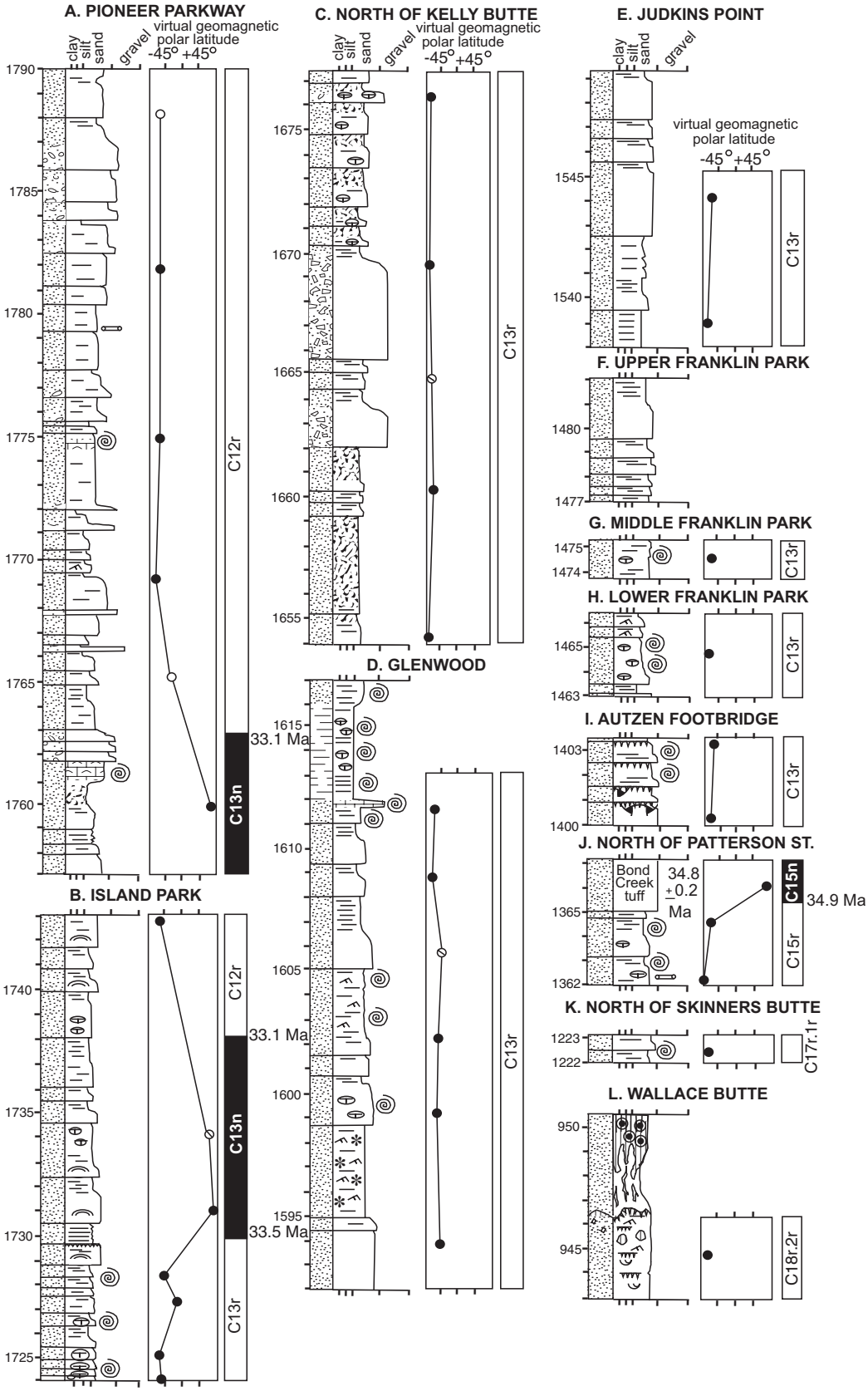

Figure 7. Sedimentological and paleomagnetic observations of marine Eugene Formation in measured sections from Wallace Butte to Springfield. Meter levels are from composite stratigraphic sections of Figure 2. All sections measured and logged by Retallack with paleomagnetic data from Prothero. Symbols are as for Figure 6.

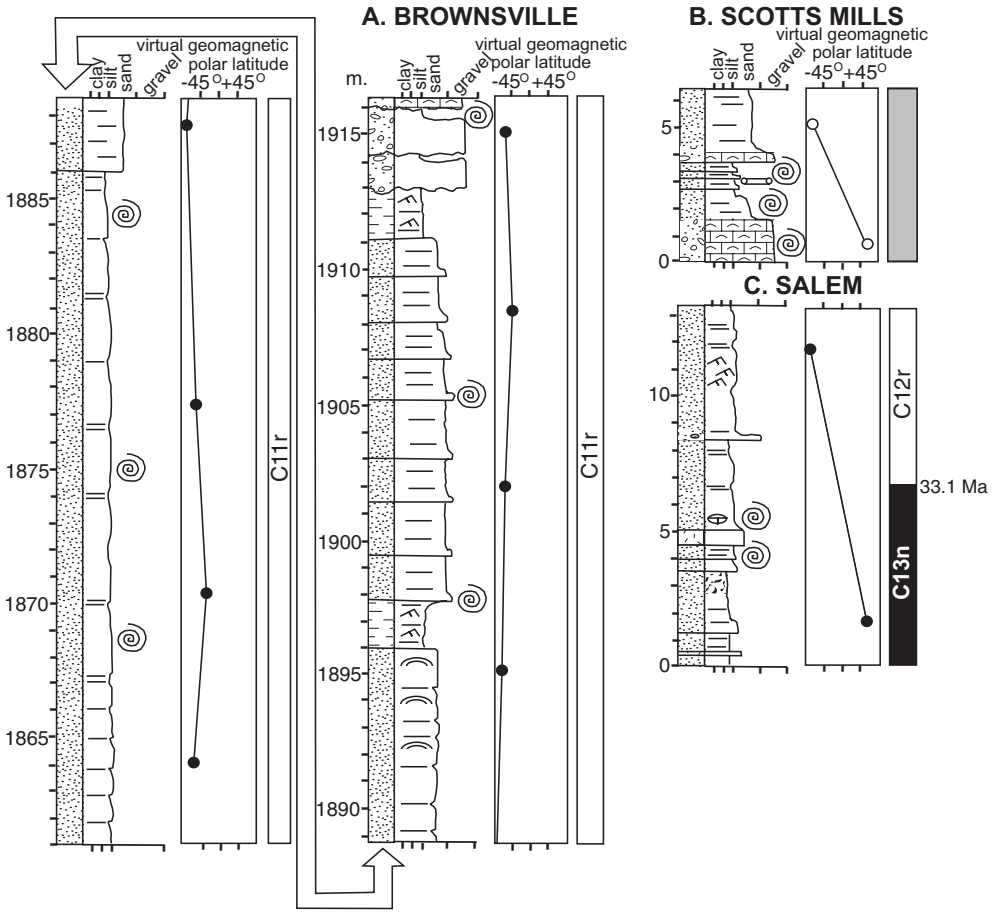

Figure 8. Sedimentological and paleomagnetic observations of Eugene Formation near Brownsville and Salem and Scotts Mills Formation near Molalla, Oregon. Meter levels at Brownsville are interpolated from nearby composite stratigraphic sections of Figure 2, but Salem and Scotts Mills sections are remote from Eugene. All sections measured and logged by Retallack with paleomagnetic data from Prothero. Symbols are as for Figure 6.

(Fig. 2; Table 2; Data Repository).[1] New radiometric ages were determined for eight specimens of tuffs from the Eugene area (Tables 2 and 3; Fig. 10) using the $^{40}Ar/^{39}Ar$ incremental heating method on plagioclase separates. Incremental heating experiments were performed at Oregon State University using MAP215/50 mass spectrometer. Samples of 50–100 mg of phenocrysts and the FCT-3 biotite monitors (standard age of 28.03 ± 0.18 Ma after Renne et al., 1994) were wrapped in Cu-foil and stacked in evacuated quartz vials and irradiated with fast neutrons for 6 hr in the core of the 1MW TRIGA reactor at Oregon State University. The measured argon isotopes (^{40}Ar, ^{39}Ar, ^{38}Ar, ^{37}Ar, and ^{36}Ar) were corrected for interfering Ca, K, and Cl nuclear reactions (McDougall and Harrison, 1999) and for mass fractionation. Apparent ages for individual temperature steps were calculated using ArArCALC software (Koppers, 2002) assuming an initial atmospheric $^{40}Ar/^{39}Ar$ value of 295.5, and reported uncertainty (2σ) includes errors in regression of peak height measurements, in fitting the neutron flux measurements (J-values), and uncertainty in the age of the monitor. Plateau ages are the average of concordant step ages, comprising most of the gas released, weighted by the inverse of their standard errors. Isochron ages, calculated from the correlation of $^{40}Ar/^{36}Ar$ versus $^{39}Ar/^{36}Ar$, are identical to plateau ages,

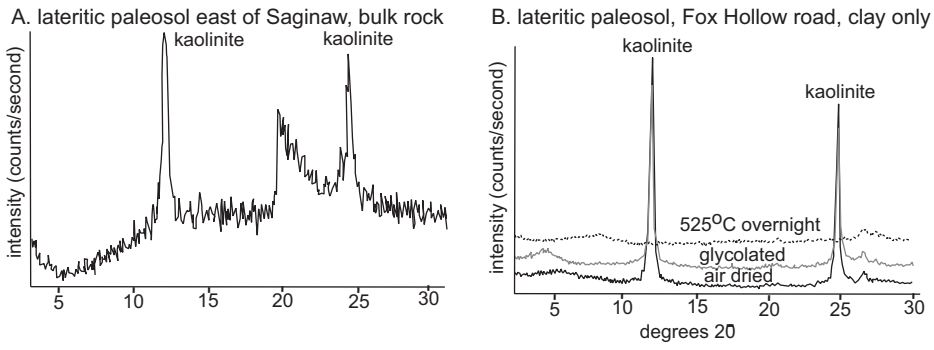

Figure 9. X-ray diffractograms of clays in paleosol marker beds in Eugene area (by Ambers).

[1]GSA Data Repository item 2004103, interpolated age of fossil floras and marine fossil localities, is available on the Web at http://www.geosociety.org/pubs/ft2004.htm. Requests may also be sent to editing@geosociety.org.

TABLE 2. RADIOMETRIC DATING NEAR EUGENE, OREGON

Dated rock	Level (m)	Age (Ma)	Coordinates
New age determinations of tuffs ($^{40}Ar/^{39}Ar$ plateau by Duncan)			
Dexter tuff 1 mile W Jasper railway siding	2352	25.9±0.6	SW¼SE¼SW¼ S10 T18S R2W Lane Co.
tuff above Willamette flora, 0.5 miile NE Goshen	1974	30.6±0.5	SE¼NW¼SE¼ S14 T18S R3W Lane Co.
Spores Point tuff on McKenzie R. at Spores Point	1830	31.3±0.6	NE¼SW¼NE¼ S10 T17S R3W Lane Co.
Mosser Mountain tuff at Short Mountain landfill	1824	31.8±0.8	NE¼NW¼NW¼ S36 T18S R3W Lane Co.
Mosser Mountain tuff 1 mile NW Buck Mountain	1824	32.3±0.6	SW¼NW¼NE¼ S14 T16S R3W Lane Co.
Bond Creek tuff on Willamette R. N of Patterson St	1365	33.9±0.7	SW¼NW¼NE¼ S32 T17S R3W Lane Co.
Bond Creek tuff on Willamette R. N of Patterson St	1365	34.8±0.2	SW¼NW¼NE¼ S32 T17S R3W Lane Co.
Fox Hollow tuff, Lorane Highway 0.5 mile W Spencer Grange	806	41.0±0.6	SE¼SE¼NW¼ S22 T18S R4W Lane Co.
Old determinations of flows and tuffs in sequence (K-Ar)			
Tuff slopes of Winberry Mountain (Millhollen, 1991)	2856	21.6±1.0	SE¼NW¼SE¼ S20 T19S R2W Lane Co.
Basalt 0.5 miles south of Mabel (Lux, 1981 #41)	2320	27.0±1.0	SE¼SW¼NE¼ S5 T16S R1W Lane Co.
Basalt 5 miles NE Springfield (Feibelkorn et al., 1982 #73)	2256	28.9±0.3	NE¼NE¼NE¼ S24 T17S R2W Lane Co.
Basalt 5 mile south of Brownsville (Lux, 1981 #32)	1832	28.9±0.5	NE¼NW¼NE¼ S25 T14S R3W Linn Co.
Basalt 0.5 miles south of Mabel (Lux, 1981 #41)	2320	28.3±1.1	SE¼SW¼NE¼ S5 T16S R1W Lane Co.
Andesite Twin Buttes, 4 mi. SW Brownsville (Lux, 1981 #30)	2256	29.7±0.4	NE¼NW¼NE¼ S22 T14S R3W Linn Co.
Basalt 1 mile south of Mabel (Lux, 1981 #40)	2300	29.7±0.8	SW¼SE¼SW¼ S5 T16S R1W Lane Co.
Basalt of Springfield Butte quarry (Lux, 1981 #42)	2256	30.3±1.1	NE¼SE¼SE¼ S2 T18S R3W Lane Co.
Tuff of Willamette flora, Goshen (Evernden & James, 1964)	1954	31.8±1.0	SE¼NW¼SE¼ S14 T18S R3W Lane Co.
Basalt on 40th and McDonald St., S Eugene (Lux, 1981 #43)	1330	32.4±0.8	SW¼SE¼SW¼ S8 T18S R3W Lane Co.
Andesite north of London (McBirney, 1978)	1100	34.3±0.5	SW¼SW¼NW¼ S20 T22S R3W Lane Co.
Basalt on 40th and McDonald St., S Eugene (Lux, 1981 #43)	1330	35.3±0.9	SW¼SE¼SW¼ S8 T18S R3W Lane Co.
Basalt 3 miles SW Cottage Grove (Lux, 1981 #22)	1100	36.2±0.5	NE¼NW¼NE¼ S12 T21S R4W Lane Co.
Basaltic andesite 3 miles S Creswell (Lux, 1981 #21)	1320	37.0±1.3	NW¼SE¼SE¼ S35 T19S R3W Lane Co.
Basaltic andesite 2 miles E Cottage Grove (Lux, 1981 #25)	1330	37.7±0.9	SE¼SW¼NE¼ S35 T20S R3W Lane Co.
Basalt 2 miles east of Creswell (Lux, 1981 #24)	1350	38.7±0.5	SW¼SW¼NE¼ S18 T19S R2W Lane Co.
Basalt 3 miles W Creswell (Feibelkorn, et al. 1982 #61)	1250	38.7±0.5	NE¼NE¼NW¼ S17 T19S R3W Lane Co.
Basalt 2 miles SE Creswell (Lux, 1981 #23)	1300	39.7±1.4	SW¼NE¼NW¼ S25 T19S R3W Lane Co.

TABLE 3. ANALYTICAL DATA FOR NEW $^{40}AR/^{39}AR$ RADIOMETRIC DATES

Sample	Total fusion age (Ma)	2σ error	Plateau age (Ma)	2σ error	MSWD	Isochron age (Ma)	2σ error	$^{40}Ar/^{36}Ar$ initial	2σ error	J
Dexter tuff	25.75	0.68	25.87	0.59	0.11	25.53	1.10	301.8	25.8	0.001612
Tuff above Willamette flora	30.86	0.49	30.64	0.51	1.83	30.68	0.78	293.6	20.6	0.001584
Spores Point tuff	30.88	0.55	31.27	0.57	0.74	31.25	0.67	296.1	12.5	0.001564
Mosser Mountain tuff	31.64	1.05	31.86	0.82	0.47	32.09	1.60	293.5	10.8	0.001591
Mosser Mountain tuff	32.88	0.66	32.26	0.60	0.29	32.20	1.05	297.0	28.7	0.001569
Bond Creek tuff	33.92	0.69	33.86	0.69	0.30	33.77	0.78	300.6	21.7	0.001539
Bond Creek tuff	34.63	0.21	34.85	0.22	1.70	34.99	0.26	277.0	19.0	0.001724
Fox Hollow tuff	40.68	0.61	40.98	0.56	0.24	41.13	0.66	279.2	38.4	0.001632

Note: All analyses used fresh plagioclase; ages calculated using biotite monitor FCT-3 (28.03 ± 0.18 Ma) and the following decay constants: $\lambda\varepsilon$ = 0.581E-10/yr, $\lambda\beta$ = 4.963E-10/yr; MSWD is the mean square of weighted deviations, an F-statistic that is significant when less than ~2.5.

and $^{40}Ar/^{36}Ar$ intercepts confirm that initial Ar was of atmospheric composition (Table 3). For further details of methods, see Duncan (2002) and Data Repository (see footnote 1).

The newly determined $^{40}Ar/^{39}Ar$ ages form a highly significant relationship with stratigraphic level (Fig. 2) that is broadly concordant with previously determined K-Ar ages (Table 2). This linear relationship can be used to interpolate the geological age of all fossil localities whose stratigraphic level is known (Fig. 2; Data Repository [see footnote 1]). Polynomial and other fits to these data proved no better than the linear fit used here.

MAGNETOSTRATIGRAPHY

Rock exposures are small and scattered in this forested and built landscape. Three oriented block samples were collected at each paleomagnetic study site. In the laboratory, samples were cored using a drill press. Small samples were cast into cylinders of Zircar aluminum ceramic. Samples were then studied by Prothero using the 2G cryogenic magnetometer with automated sample changer at the California Institute of Technology. After natural remnant magnetization was measured, each sample was demagnetized in alternating fields of 25, 50, and 100 Gauss to determine coercivity behavior and eliminate multidomain remanences before they were baked in. Each sample was then thermally demagnetized at 300, 400, 500, and 600 °C to remove remanence held in high-coercivity iron hydroxide such as goethite (which dehydrates at 200 °C) and also to determine how much remanence derived from above the Curie point of magnetite (580 °C).

About 0.1 g of powdered samples of representative lithologies were placed in epindomorph tubes and subjected to increased isothermal remnant magnetization to determine their saturation behavior. These samples were

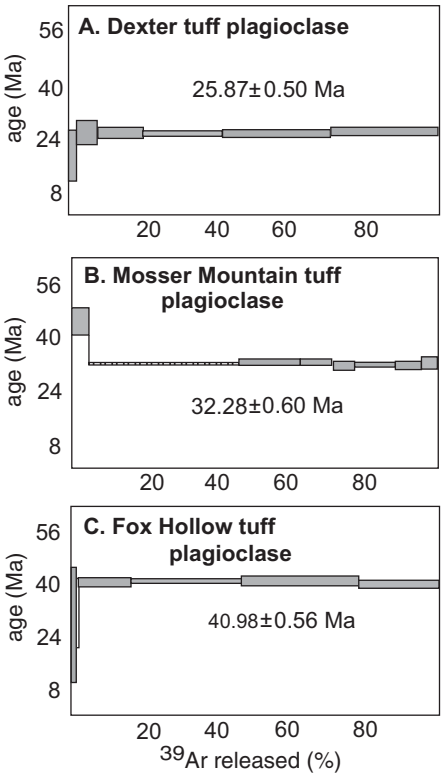

Figure 10. $^{40}Ar/^{39}Ar$ incremental heating age determinations of selected tuffs in Eugene area (by Duncan).

also twice demagnetized in alternating fields, once after an isothermal remnant magnetization in a 100-mT peak field was acquired and once after anhysteritic remnant magnetization was acquired on a 100-mT oscillating field (Pluhar et al., 1991). Such data are used for the modified Lowrie-Fuller test shown in Figure 11.

Orthogonal demagnetization ("Zijderveld") plots of representative samples are shown in Figure 12. In almost every sample there was significant response to alternating field magnetization, showing that the remanence is held in a low-coercivity mineral such as magnetite. In addition, nearly every sample lost its remanence above the Curie temperature (580 °C) of magnetite, confirming that it was the primary carrier of the remanence. Most samples (Fig. 12A–D) showed a single component of remanence that was clearly oriented in a normal or reversed direction (after dip correction) and decayed steadily to the origin with no apparent overprinting. A few samples (Fig. 12E) had a normal overprint that was removed by alternating field demagnetization and showed a stable remanence that decayed toward the origin at demagnetization steps of 300 °C.

Isothermal remanent magnetization saturation curves (Fig. 11) showed that the samples did not completely reach saturation at 300 mT (millitesla), suggesting that both magnetite and hematite are present. In all samples, the anhysteretic natural magnetization was more resistant to alternating field demagnetization than the isothermal remanent magnetization, showing that the remanence is held in single-domain or pseudo-single-domain grains.

Because most of the samples showed a single component of magnetization, that component was summarized using the least squares method of Kirschvink (1980). All three vectors from each site were then combined using the methods of Fisher (1953), and sites were ranked statistically according to the scheme of Opdyke et al. (1977). These site statistics are plotted as virtual geomagnetic polar latitudes in Figures 6–8.

Although there was some dip variation across the region, dips were less than 12°, not steep enough to conduct a fold test. However, the means for the normal sites (D = 17.0, I = 49.2, k = 34.1, α_{95} = 10.5) and those for reversed sites (D = 196.8, I = –63.3, k = 17.3, α_{95} = 6.3) are antipodal within error estimates (Fig. 13). Thus, overprinting has been removed, and the directions are a primary or characteristic direction. These data pass a Class A reversal test of McFadden and McElhinny (1980; γ_c = 4.7°).

The Eugene, Fisher, and Scotts Mills Formations show slight clockwise rotation when compared with the Eocene cratonic pole of Diehl et al. (1983) and correcting error estimates as suggested by Demarest (1983). This is apparent from comparison with our Eocene paleopoles and the current pole (Fig. 13), which is corrected for secular variation over the last 6000 yr from Fish Lake, Oregon (Hagee and Olson, 1989). We have not found the 29° ± 11° tectonic rotation noted by Wells (1990) from the 30.3 Ma intrusion at Skinner Butte, which is geographically (Fig. 1) and temporally (Fig. 3) central to our study sequence. Up to 74° of post-Eocene clockwise tectonic rotation is found in coastal blocks of the Pacific Northwest (Prothero and Hankins, 2001), but post-Eocene rotation declines to10–18°, close to our error envelopes, within the Cascades and Klamath Mountains (Wells, 1990).

Paleomagnetic interpretation of these scattered exposures (Figs. 6–8) would not have been conclusive without supporting radiometric dating and physical stratigraphic relationships to marker

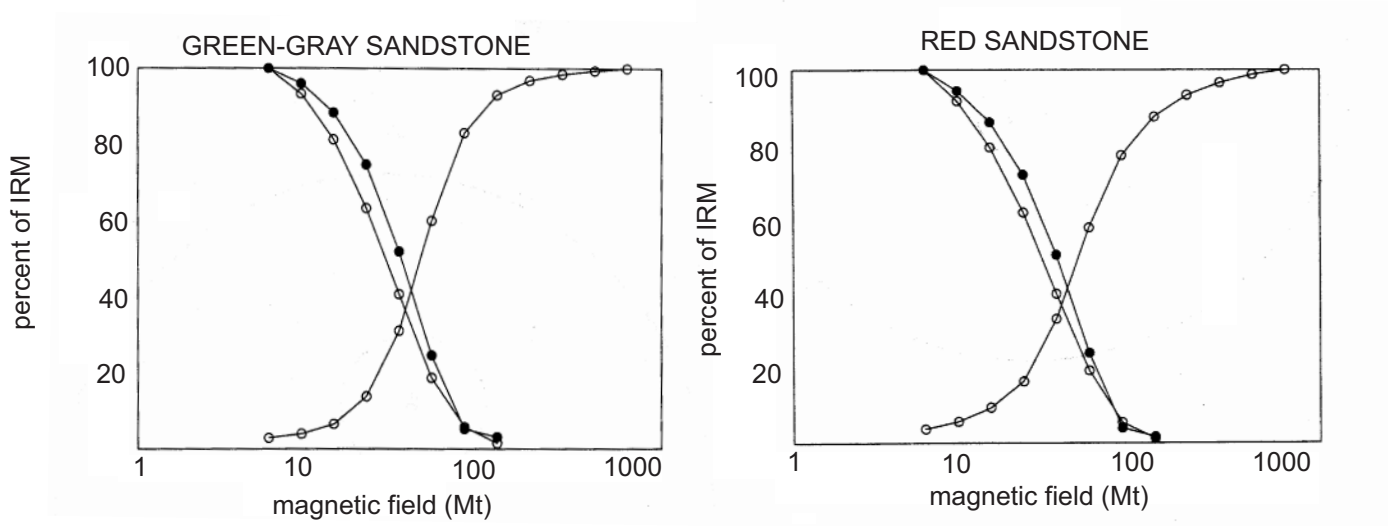

Figure 11. Isothermal remanent magnetic acquisition (ascending curves on right) and Lowrie-Fuller test (two descending curves) for representative samples from Eugene area (by Prothero). Open circles are isothermal remanent magnetization and solid circles are anhysteretic remnant magnetization.

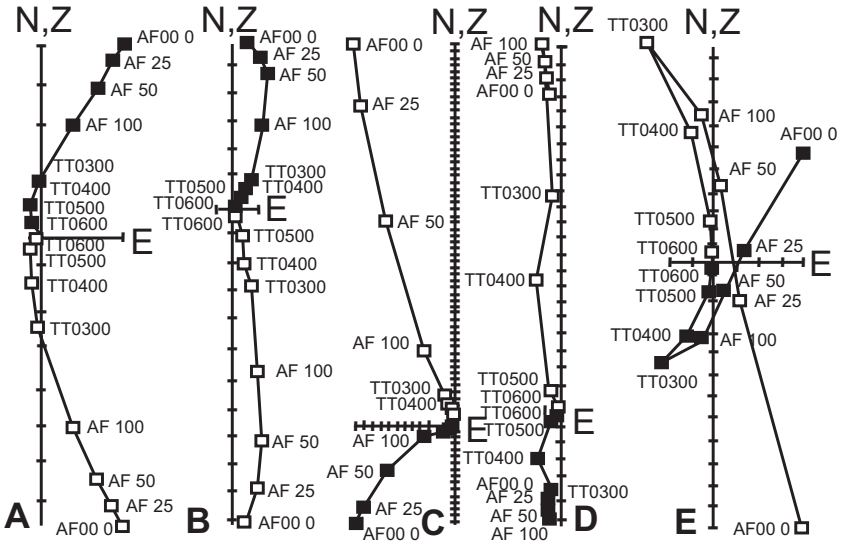

Figure 12. Orthogonal demagnetization ("Zijderveld") plots of representative sedimentary rocks in Eugene area (by Prothero). Solid squares indicate horizontal component, and open squares indicate vertical component. AF is alternating field step (in gauss), TT is thermal step (°C), and each division is 10^{-4} A/m.

tuffs. The paleomagnetic reversal (34.9 Ma) associated with the Bond Creek tuff on the Willamette River north of Patterson (Fig. 7J) offers striking confirmation of its radiometric dating at 34.8 ± 0.2 Ma. Especially useful paleomagnetic observations include those of the Goshen flora overlying a reversal at 33.5 Ma (Fig. 6I) but which is estimated to be 33.4 Ma from radiometric interpolation (Fig. 2), confirming that it is above the Eocene-Oligocene boundary at 33.7 Ma (Berggren et al., 1995). Also confirmed is the Eocene (39.6 Ma) age of the reversal above the main (upper) Comstock flora (Fig. 6J), which again is close to the flora's radiometric interpolation age of 39.7 Ma (Fig. 2).

Our paleomagnetic examination of sites outside the mapped area, such as reversed polarity for the Scotts Mills Formation (Fig. 8B), offers no better resolution than biostratigraphy within the zone of *Liracassis apta* (Miller and Orr, 1987; Linder et al., 1988), as late Oligocene C6C.3r to C9r, or 24.73 to 28.28 Ma (Cande and Kent, 1995). The reversal observed south of Salem (Fig. 8C) can be more precisely determined as early Oligocene (33.1 Ma) due to tighter biostratigraphic control of late Refugian benthic foraminifera (McKillip, 1992). Other marine fossil localities near Salem (Hickman, 1969; Smith-Gharet, 1999) also are Oligocene.

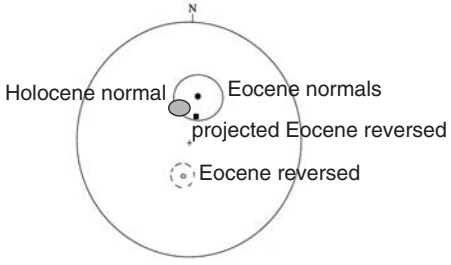

Figure 13. Stereonet showing mean and ellipse of confidence for normal sites (solid circle), and reversed sites (open circle) from Eugene (by Prothero). Solid square is projection of reversed mean onto lower hemisphere and is a successful reversal test for magnetic signal in sedimentary rocks of Eugene. Gray ellipse is modern field direction averaged for last 6000 yr using data from Fish Lake, Oregon (Hagee and Olson, 1989).

FOSSIL PLANT EXTINCTIONS

Fossil plant assemblages of several distinct floras have been found in the Eugene area and are interpreted as representing the transition from tropical warm evergreen (Kummerian) to temperate cool deciduous (Angoonian) floras (Wolfe, 1981a, 1994, 1995). Our compilation shows overturn of species above the Eocene-Oligocene boundary, so that Kummerian and Angoonian floras share few species (Figs. 14 and 15; Data Repository [see footnote 1]). The early Oligocene Goshen flora (33.4 Ma) has the highest diversity and greatest number of originations, but peaks of extinctions follow at 33 and 29 Ma, and there is a large diversity rebound at 31 Ma. Floral overturn is thus an abrupt change into a fluctuating but generally downward ramp of diversity lasting 6 m.y. after the Eocene-Oligocene boundary until a new late Oligocene floral equilibrium. The geological setting and paleoecology of this floral transition are discussed in the following paragraphs.

Eocene Tropical (Kummerian) Floras

The Kummerian Stage is based on fossil floras from the upper part of the Puget Group of southeastern Washington but includes floras from at least 13 localities in Alaska (Wolfe, 1968, 1981b; Ridgway et al., 1995) and the Comstock (Sanborn, 1935) and Hobart Butte floras (Hoover, 1963) south of Cottage Grove (Fig. 1). The Comstock flora, dated here by tephrostratigraphy (Fig. 1) and magnetostratigraphy (Fig. 6J) at 39.6 Ma, is preserved as impressions associated with Entisols and fluvial paleochannels (Fig. 6J), indicating that it was riparian fringe vegetation. This taphonomic setting emphasizes deciduous broadleaved angiosperms over evergreen angiosperms and conifers (Wolfe, 1981a). This setting is comparable to other late Eocene floras dominated by the plane tree *Macginitea angustiloba*, such as the flora of lahars and Entisols of the Clarno Formation (Manchester, 1986; Retallack et al., 2000). Like the Clarno floras, the Comstock and Hobart Butte floras have many thermophilic taxa such as *Liquidambar*. Neither flora has been exhaustively collected.

The Peaceful Valley, Bear Creek, and Scotts Valley floras are stratigraphically below the Comstock flora but have not been studied in detail. They are old enough to belong to Wolfe's (1977, 1981b) Ravenian or Fultonian stages, both of which are considered to be older than 37 Ma by Wolfe et al. (1998). Our new dates on the main (upper) Comstock flora at 39.6 Ma and the 40 Ma Fox Hollow tuff overlying the lower Comstock flora (both floras regarded as Kummerian by Wolfe, 1981b) indicate that the Kummerian-Ravenian boundary is closer to 40 Ma than 37 Ma.

Oligocene Riparian (Goshen-type) Floras

The Goshen flora has been well known since the monograph of Chaney and Sanborn (1933). Part of the reason it attracted so much attention is its stunning preservation as dark brown leaf impressions with clear venation in yellow to white tuffaceous siltstones (Fig. 14A and B), but unfortunately it lacked cuticle that could be prepared. Highway construction in 1987 exposed leaf-bearing siltstones overlying and interbedded with thick paleochannel sandstones. Many of the leaves are rolled and crumpled as in a leaf litter. The leaves are concentrated within 20 cm of planar-bedded tuffaceous siltstone overlying massive

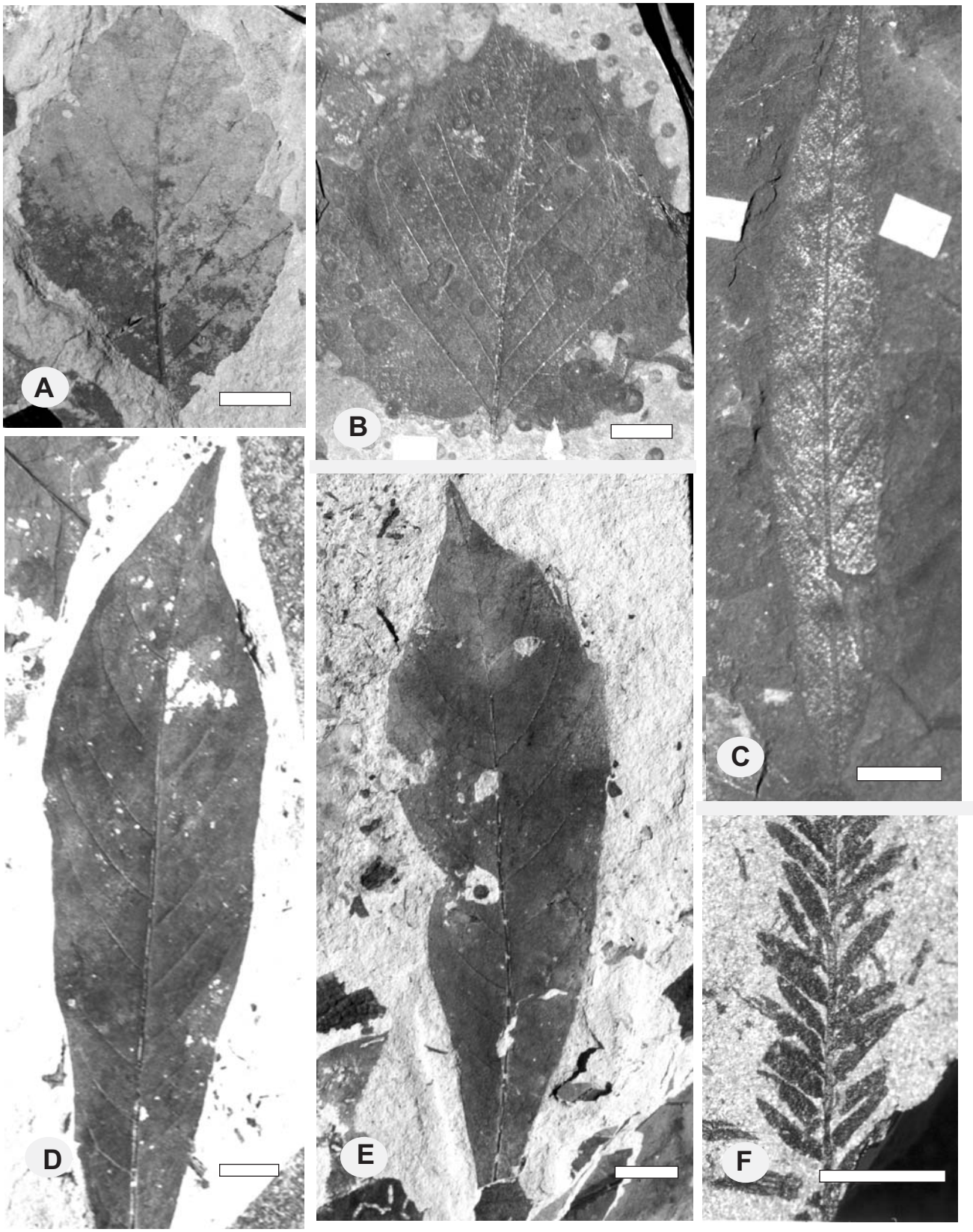

Figure 14. Selected fossil plants of Eugene area, Oregon: (A) *Alnus heterodonta* from Rujada flora; (B) *Platanus condoni* from Willamette flora; (C) *Quercus consimilis* from Willamette flora; (D) *Laurophyllum merrilli* from Goshen flora; (E) *Meliosma goshenensis* from Goshen flora; (F) *Metasequoia* sp. cf. M. *foxii* from Springfield flora. Condon Collection specimen numbers are F36217–36222, respectively. Scale bars are all 1 cm.

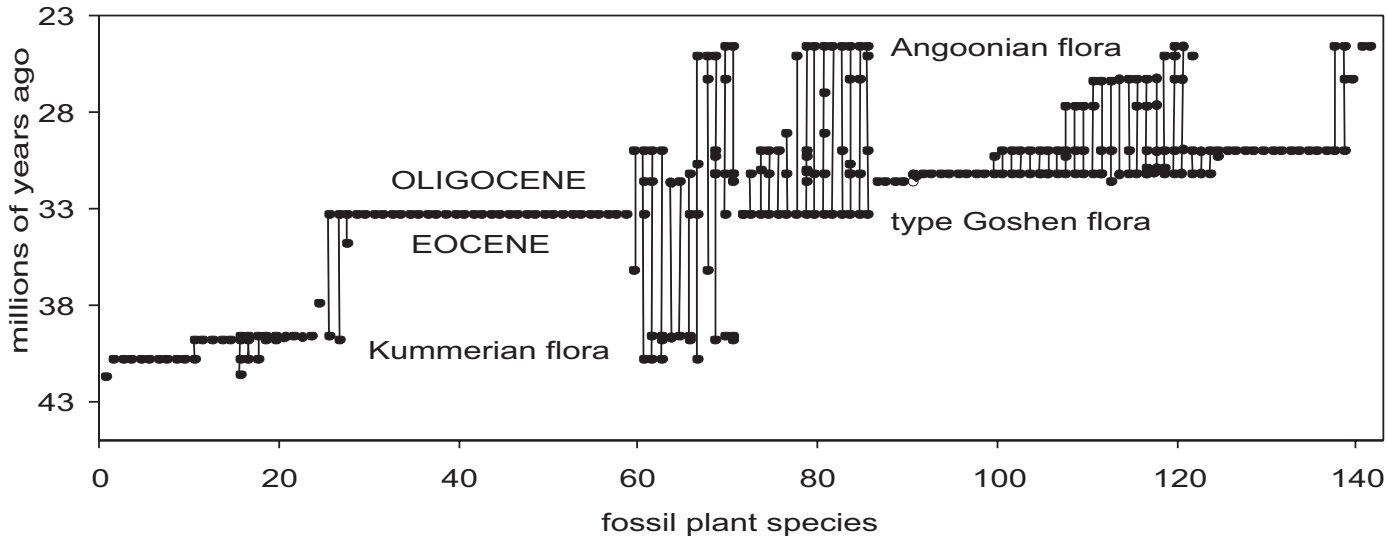

Figure 15. Stratigraphic range of Eocene and Oligocene fossil plant taxa and fossil floras near Eugene, Oregon. 1-*Carya* sp., 2-*Anona coloradensis*, 3-*Aporosa pattersoni*, 4-*Viburnum variabilis*, 5-*Lonchocarpus oregonensis*, 6-*Lonchocarpus standleyi*, 7-*Mallotus oregonensis*, 8-"*Persea" praelingue*, 9-*Pterospermum praeobliquum*, 10-*Rhamnites marginatus*, 11-*Dracontomelon sanbornae*, 12-*Liquidambar californicum*, 13-*Potamogeton* sp., 14-*Quercus nevadensis*, 15-*Thouinopsis myricaefolia*, 16-*Litseaphyllum similis*, 17-*Platanus comstocki*, 18-*Polyaltha chaneyi*, 19-*Macginitea angustiloba*, 20-*Joffrea spiersii*, 21-*Litseaphyllum praesamarensis*, 22-*Asplenium primero*, 23-*Asplenium hurleyensis*, 24-*Rhamnus calyptus*, 25-*Calkinsia franklinensis*, 26-*Cordia rotunda*, 27-*Anemia delicatula*, 28-*Cupania packardi*, 29-*Callichlamys zeteki*, 30-*Calyptranthus arbutifolia,* 31-*Camelia oregona*, 32-*Aristolochia mexiana*, 33-*Chrysobalanus ellipticus*, 34-*Cupania oregona*, 35-*Dillenites* sp., 36-*Diospyros oregona*, 37-*Drimys americana*, 38-*Ficus plinerva*, 39-*Ficus quisumbingi*, 40-*Hydrangea russelli*, 41-*Inga oregona*, 42-*Laurophyllum merrilli*, 43-*Litseaphyllum presanguinea*, 44-*Lucuma* sp., 45-*Lucuma standleyi*, 46-*Magnolia hilgardiana*, 47-*Magnolia reticulata*, 48-*Meliosma goshenensis*, 49-"*Phyllites" gosheni*, 50-"*Phyllites" lanensis*, 51-*Psychotria oregona*, 52-*Quercus howei*, 53-*Quercus lanensis*, 54-*Sapium standleyi*, 55-*Siparuna ovalis*, 56-*Strychnos* sp., 57-*Symplocos oregona*, 58-*Viburnum eocenicum*, 59-*Viburnum palmatum*, 60-*Palaeophytocrene* sp., 61-*Koelreuteria mixta*, 62-*Magnolia californica*, 63-*Calkinsia dilleri*, 64-*Alnus operia*, 65-*Dryopteris lesquereuxi*, 66-*Cyathea pinnata*, 67-"*Ficus" goshenensis*, 68-*Pinus* sp., 69-*Pterocarya mixta*, 70-*Lithocarpus klamathensis*, 71-*Equisetum oregonense*, 72-*Siparuna standleyi*, 73-*Anona prereticulata*, 74-*Florissantia speirii*, 75-*Pflafkeria obliquifolia*, 76-*Smilax goshenensis*, 77-*Lindera oregona*, 78-*Meliosma rostrata*, 79-*Allophylus wilsoni*, 80-*Cordia oregona*, 81-*Fagus oregona,* 82-*Grewiopsis dubium*, 83-*Meliosma aesculifolia*, 84-*Ocotea ovoidea*, 85-*Platanus macginitei*, 86-*Cinnamomophyllum eocernuum*, 87-*Woodwardia* cf. *W. columbiana*, 88-*Tabernaemontana chrysophylloides*, 89-*Colubrina* sp., 90-*Celastrus* sp., 91-*Zelkova browni,* 92-*Tsuga sonomensis*, 93-*Sophora* sp., 94-*Pseudotsuga laticarpa*, 95-*Osmunda occidentale*, 96-*Machilus asiminoides*, 97-*Fraxinus coulteri*, 98-*Cyperacites* sp., 99-*Cephalotaxus* sp., 100-*Terminalia oregona*, 101-*Metasequoia* sp., 102-*Platanus dissecta*, 103-*Pinus johndayensis*, 104-*Mahonia simplex*, 105-*Juglans* sp., 106-*Fothergillia preovata*, 107-*Crataegus merriami*, 108-*Cunninghamia chaneyi*, 109-*Castanea basidentata*, 110-*Abies* spp., 111-*Pyrus oregonensis*, 112-*Exbucklandia oregonensis*, 113-*Cercidiphyllum crenatum*, 114-*Salix schimperi*, 115-*Keteeleria rujadana*, 116-*Castanopsis longifolium*, 117-*Betula angustifolia*, 118-*Quercus consimilis*, 119-*Palaeocarya* sp., 120-*Sequoia affinis*, 121-*Rhus varians*, 122-*Platanus condoni*, 123-*Ulmus* sp., 124-*Alnus heterodonta*, 125-*Cruciptera simsoni*, 126-*Acer manchesteri*, 127-*Aralia* sp., 128-*Arbutus* sp., 129-*Berchemia* sp., 130-*Cedrela merrilli*, 131-*Cercis maurerae*, 132-*Chamaecyparis* sp., 133-*Ginkgo adiantoides*, 134-*Glyptostrobus oregonensis*, 135-*Platanus exaspera,* 136-*Tetraclinis potlatchensis*, 137-*Torreya*, 138-*Folkeniopsis praedecurrens*, 139-*Hydrangea* sp. cf. *H. bendirei*, 140-*Pterocarya orientalis*, 141-*Phoebe oregonensis*, 142-*Prunus pristina* (data from Chaney and Sanborn, 1933; Sanborn, 1935; Brown, 1950, 1959; LaMotte, 1952; Lakhanpal, 1958; Vokes et al., 1951; Hoover, 1963; Wolfe, 1968, 1977; Tanai and Wolfe, 1977; Crane and Stockey, 1985; Wolfe and Tanai, 1987; Doyle et al., 1988; Manchester, 1986, 1992; Meyer and Manchester, 1997; Myers et al., 2002).

siltstone containing sparse carbonized fossil root traces that is interpreted as a riparian Entisol overwhelmed by flooding. These observations suggest that the Goshen flora was riparian like the Comstock flora. The Goshen flora is diverse (48 spp.) but dominated by aguacatilla (*Meliosma goshenensis*; Fig. 14E) with common laurel (*Litseaephyllum presanguinea*) and fig ("*Ficus*" *quisumbingi*: 10% or more of collection of Chaney and Sanborn, 1933; with names emended by Wolfe, 1977; Doyle et al., 1988).

The Sweet Home floras also have been regarded as Goshen-type floras (Wolfe, 1981b), and like the Goshen flora, they have large leaves with drip tips, including aguacatilla (*Meliosma aesculifolia*) and soapberry (*Allophyllus wilsoni*; Peck et al., 1964). Sweet Home floras are dominated by *Prunus pristina* at north Sweet Home (Brown, 1959) and *Platanus condoni* at south Sweet Home (Table 3). This may be in part a taphonomic artifact, because these floras are fossil leaf litters in near-stream facies overwhelmed by the Dexter tuff. Their paleosols include abundant permineralized wood that is especially well known near Holley (Richardson, 1950; Brown, 1950, 1959; Gregory, 1968). Such fossil floras preferentially sampled individual trees growing nearby and need to be collected some distance along strike to obtain a flora as regionally representative as flora that is washed and blown into a lake.

Other Goshen-type floras include the Russel Creek, Greentop, and Coburg floras. Leaves and

a dragonfly wing from Russel Creek were collected by Washburne (1914; Fraser, 1955). The Russel Creek flora includes magnolia (*Magnolia californica*) and soapberry (*Allophyllus wilsoni*), linking it with the type Goshen flora, but in addition it has alder (*Alnus* sp.) and katsura (*Cercidiphyllum* sp.: Vokes et al., 1951), which links it with Angoonian floras (of Wolfe, 1981b). The Coburg (Myers et al., 2002) and Greentop floras (Table 3) are additional Goshen-type floras discovered during this study. The Russel Creek and Greentop fossils are oxidized impressions, but the Coburg flora has impressions that are potentially amenable to cuticular analysis (as outlined by Kerp and Krings, 1999). Coburg and Greentop floras are fossil leaf litters atop weakly developed paleosols (Entisols), which include permineralized fossil stumps (Fig. 6F *in* Myers et al., 2002). Both contain laurels (*Ocotea ovoidea*) like the Goshen flora, as well as sycamore (*Platanus condoni*), alder (*Alnus heterodonta*), and Malayan aspen (*Exbucklandia oregonensis*), which links them floristically with Angoonian floras.

Beyond the mapped area, Goshen-type floras include the Scio (Sanborn, 1949) and Bilyeu Creek (Klucking, 1964) floras of Oregon; floras of the Ohanapecosh, Fifes Peak, and Stevens Ridge Formations in Washington (Wolfe, 1981b); the La Porte flora of California (Potbury, 1935; Doyle et al., 1988); and the Rex Creek flora of Alaska (Wolfe, 1992; Ridgway et al., 1995). Dating of these floras suggests that Goshen-type floras are mainly Oligocene riparian communities, distinct from the coeval lacustrine Angoonian floras. Our radiometric dating (Fig. 2) and magnetostratigraphy (Fig. 3) indicate that the type Goshen flora is earliest Oligocene (33.4 Ma). The Russel Creek and Coburg floras are also early Oligocene (31.2 Ma and 31.3 Ma, respectively). The Sweet Home and Greentop floras are late Oligocene (24.7 Ma and 21.7 Ma, respectively). Fossil floras of the Ohanapecosh, Fifes Peak, and Stevens Ridge Formations in Washington are radiometrically dated by K-Ar at 34.9 ± 1.2 Ma (Fischer, 1976) and 30.8 ± 3 Ma (Laursen and Hammond, 1974). Also comparable is the La Porte flora of California (Wolfe, 1981b), which was dated at 33.4 Ma using K-Ar (by Evernden and James, 1964; corrected using Dalrymple, 1979; flora after Wolfe et al., 1998). Goshen-type floras are a floral facies rather than a floral biozone (Myers, 2003), as suspected by Wolfe (1981b). Palynological zonation of the Alaskan Eocene-Oligocene transition recognizes two palynozones that are correlated with Kummerian and Angoonian floral zones, but thermophilic pollen such as Japanese spurge (*Pachysandra*) and Malaya beam (*Engelhardtia*) persist into Angoonian assemblages (Ridgway et al., 1995).

Oligocene Lacustrine (Angoonian) Floras

The Angoonian Stage was established for Alaskan fossil floras (Wolfe, 1977, 1992) but includes the Rujada and Willamette floras near Eugene (Wolfe, 1981b). Only the Rujada flora has been adequately monographed (Lakhanpal, 1958), but species of the Willamette flora have been listed by Brown (for Vokes et al., 1951) and by Myers et al. (2002). The Rujada flora fossils are gray impressions that are variably oxidized to brown and red by weathering in outcrop (Fig. 14A). Willamette flora leaf fossils are black compressions in black shale (Fig. 14, B and C), which superficially appear to be promising for cuticular study of the kind outlined by Kerp and Krings (1999). Unfortunately, mesophylls of Willamette leaves have been extensively replaced by the zeolite mineral laumontite in a form of preservation similar to that of leaves from Cretaceous volcaniclastic rocks of the Antarctic peninsula (Jefferson, 1982). Rujada, Willamette, Lowell, and Coburg Hills floras are all in laminated lacustrine shales (e.g., Fig. 3G). These units appear varved in places but have normally graded tuffaceous beds ranging in thickness from 2 to 200 mm rather than the narrow millimetric range found in varved shales. Settling of thin tuffs is thus a competing explanation to the usual spring-thaw explanation of varved shale. A lacustrine interpretation is compatible with the discovery of fossil salamanders (*Palaeotaricha oligocenica*) along with the Willamette flora (van Frank, 1955) and caddis fly cases of *Metasequoia* needles (ichnogenus *Folindusia* of Boucot, 1990) with the Lowell flora. The Rujada (42 spp.) and Willamette flora (40 spp.) are dominated by oak (*Quercus consimilis*, Fig. 13C) and alder (*Alnus heterodonta,* Fig. 13A), which are represented by acorns and catkins as well as leaves.

Poorly known Angoonian floras include the Jasper (identifications of J.A. Wolfe tabulated by Peck et al., 1964) and Coburg Hills floras (Bristow, 1959). Beyond the mapped area (Fig. 1), Angoonian floras include the Lyons flora east of Salem (Meyer, 1973), the Thomas Creek flora southeast of Salem (Eubanks, 1962; Klucking, 1964), and the Cascadia flora near Moose Mountain east of Sweet Home (Peck et al., 1964). Of comparable age are the Trail Crossing and Canal floras near Madras (Ashwill, 1983; Smith et al., 1998) and the Bridge Creek floras of the John Day Fossil Beds and neighboring areas of central Oregon (Meyer and Manchester, 1997). In addition to megafossils (Wolfe, 1977, 1981b), Alaskan Angoonian floras can be recognized through palynology and coal petrography (Ridgway et al., 1995), and British Columbian Angoonian floras can be recognized through palynology (Rouse and Matthews, 1979).

MARINE FOSSIL EXTINCTIONS

Marine fossils of the Eugene Formation include shark teeth, seashells, and crab carapaces in hard, green-gray sandstone of deep excavations or within siderite nodules (Rathbun, 1926; Hickman, 1969; Welton, 1972). Many fossils are deeply weathered of original shell, leaving molds and casts, and others have been thermally altered and replaced by the zeolites analcime, heulandite, and stilbite (Staples, 1965). Shells do not tumble intact from friable matrix as in classical Cenozoic mollusc localities of the North American Atlantic and Gulf coasts. Lower Eugene Formation molluscs correlate with the *Echinophoria dalli* and *E. fax* zones of the Galvinian stage (Addicott, 1981; Armentrout, 1981), *Molopophorus gabbi* and *M. stephensoni* zones (Durham, 1944), *Acila shumardi* zone (Schenk, 1936), and the Eocene-Oligocene "turnover fauna" of Hickman (2003). The upper Eugene Formation has an "Oligocene recovery fauna" (Hickman, 2003) that is best referred to the *Liracassis rex* zone of the Matlockian stage (Addicott, 1981; Armentrout, 1981; Squires, 2003). Our compilation (Figs. 16–18) indicates that marine invertebrate diversity reached a peak at localities near Judkins Point (34.4 Ma) but had declined little in Glenwood (33.2 Ma), which postdated the Eocene-Oligocene boundary (33.7 Ma). Glenwood localities show a modest peak in originations (Fig. 19C). Extinctions continued until 31 Ma as an artifact of local marine regression. Marine extinctions are less drawn out than floral extinctions and broadly synchronous with the first wave of plant extinctions. The faunas involved in these extinctions are outlined in the following paragraphs.

Eocene Tropical (Cowlitz-Coaledo) Fauna

A new marine fossil locality was discovered during the 1996 excavation of the Hyundai factory southeast of Oak Hill (Figs. 16 and 18). Neither its molluscs nor lithology are comparable with those of the Eugene Formation and instead indicate that these rocks are best mapped with the Spencer Formation. This new fauna is most like those of the Coaledo Formation of southern coastal Oregon and the Cowlitz Formation of the northern Oregon and Washington coast ranges (Weaver, 1942).

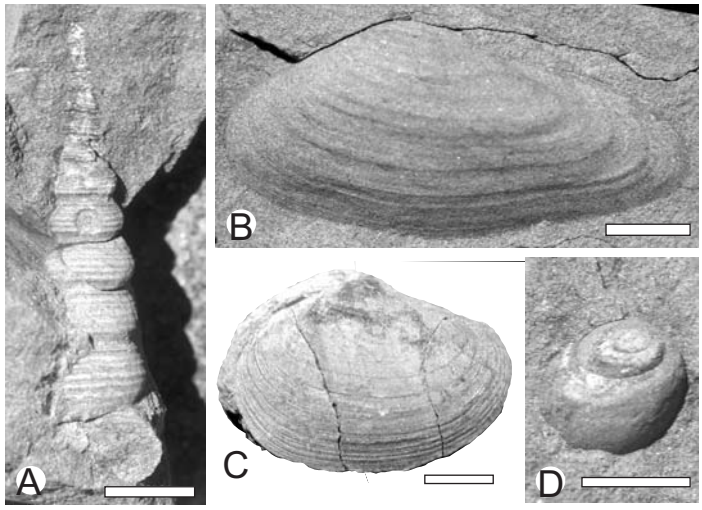

Figure 16. Selected fossil molluscs of middle to late Eocene Cowlitz-Coaledo fauna of Spencer Formation from excavations for Hyundai factory southeast of Oak Hill, west Eugene (specimen numbers are for Condon Collection, University of Oregon). (A) *Turritella uvasana* (F36232A); (B) *Yoldia olympiana* (F36235); (C) *Pitar californiana* (F36237A); (D) *Polinices nuciformis* (F36233). Scale bars all 1 cm.

A few long-ranging fossil molluscs have been found in sandstones of the Oak and Crabtree Hills at this stratigraphic level (Hickman, 1969), but the new fauna is more diverse and found in dark gray micaceous siltstones with limited bioturbation. This facies probably represents an open-marine continental shelf environment away from beaches and lagoons.

Turnover (Galvinian) Fauna

Fossil molluscs of the lower Eugene Formation (Fig. 17) have long been recognized as distinct from other Pacific coastal faunas of North America (Hickman, 1969). Much of this difference is due to very shallow marine habitats such as shallow offshore sandstones with sand dollars (*Kewia* sp.: Burns and Mooi, 2003), nearshore beach sandstones with large surf clams (*Spisula eugenensis*: Fig. 17A), and intertidal claystones with burrowing clams (*Solena eugenensis*, Fig. 17C, and *Macoma vancouverensis*, Fig. 17I) in life position (Fig. 7). These taxa and the marine snail (*Brucklarkia vokesi*, Fig. 17J) and slipper shell (*Crepidula ungana*, Fig. 17K) are the most common and widely distributed elements of the Eugene fauna. Siderite nodules contain a variety of shallow marine to intertidal crabs, including ghost shrimp (*Callianassa oregonensis*: Fig. 17F), mud crab (*Raninoides washburnei*: Fig. 17E) and swimmer crab (*Megokkos magnaspina*: Fig. 17D, Schweitzer and Feldman, 2000). Foraminifera of the Eugene Formation also indicate water depths of less than 30 m (McDougall, 1980).

The most diverse faunas of the Eugene Formation include rare molluscs of subtropical affinities, such as cockle (*Anadara* sp.), mussel (*Modiolus eugenensis*), cone shell (*Conus armentrouti*; Fig. 17H–I), and fig shell (*Ficus modesta*; Fig. 17G). These thermophilic taxa were found mostly in localities between the University of Oregon and Glenwood (35–34 Ma). These are also the most heavily collected parts of the formation, in part because they have the most interesting and diverse fauna and in part because of excavation for construction on campus.

Oligocene Recovery (Matlockian) Fauna

Oligocene marine faunas of the upper Eugene Formation share many taxa with Eocene faunas of the lower part of the formation, as shown by a low rate of originations (Fig. 19C). Nevertheless, there are some distinctive Oligocene elements, especially among fossil crabs in concretions, which include *Persephona bigranulata, Zanthopsis vulgaris,* and *Calappa laneensis* at Springfield (railway) Junction, less than a mile east of Glenwood (Rathbun, 1926). Oligocene marine faunas are best known from the uppermost part of the Eugene Formation between Brysons Quarry and Pierce's Creek in the foothills of the northern Coburg Hills, where they include bryozoans (*Membranipora*, *Terria, Idmonea)*, brachiopods (*Eohemithyris alexi, Terebratalia transversa, Terebratulina tejonense*), limpets (*Acmea dickersoni, A. mitra*), and scallops (*Chlamys cowlitzensis, C. grunskyi, C. washburnei*; Shroba, 1992). These taxa are unknown in the lower Eugene Formation, but some are known elsewhere in Eocene rocks of the Pacific Northwest, and only one of the brachiopods (*T. transversa*) and one of the limpets (*A. mitra*) are likely new evolutionary appearances (Weaver, 1942; Hertlein and Grant, 1944; Addicott, 1981). In addition, the *Acila shumardi* lineage of clams is the most prominent of a variety of newly appearing cold-water elements of likely Asiatic origin (Hickman, 2003). The Oligocene recovery fauna has low diversity and particularly lacks thermophilic and offshore marine taxa. Its gravels and barnacle coquinas probably accumulated along a rocky coast with pocket beaches like that documented for the Scotts Mills Formation near Salem (Miller and Orr, 1987).

PALEOCLIMATIC CHANGE

Chaney and Sanborn's (1933) pioneering study of the Goshen flora noted the surprisingly tropical paleoclimatic implications of its leaf size and margin type. For example, leaves with attenuate apices (or drip tips, as in *Meliosma*, Fig. 14E) are found in rainy climates (Givnish, 1987). Leaves with a dentate margin (as in *Alnus*, Fig. 14A) are more common in cool climates than entire-margined leaves, probably because dissection increases the thickness of the boundary layer impeding heat flow out of the leaf (Gurevitch, 1988). An advantage of this kind of paleoclimatic interpretation is its independence from taxonomic assignments, although it is sensitive to the number of species recognized (Wolfe, 1993; Gregory, 1994). The approach is not without problems related to taphonomy (Greenwood, 1992; Spicer and Wolfe, 1987; Myers, 2003), past atmospheric CO_2 levels (Gregory, 1996), and how assemblages are grouped geographically (Dolph, 1979, Dolph and Dilcher, 1979). This kind of inference has now been codified within a computer program called Climate Leaf Analysis Multivariate Program (CLAMP) (Wolfe, 1993, 1995; Wolfe et al., 1998; Wolfe and Spicer, 1999), which estimates mean annual temperature (MAT), mean annual range of temperature (MART), and mean annual precipitation (MAP) from leaf physiognomic data. All the floras studied in this way from the Eugene area were near sea level, so lapse rate calculations are not needed (Wolfe et al., 1998). The temperature decline and increase in seasonal temperature variation between the Goshen and Rujada-Willamette floras remain (Table 4) but are here dated after the Eocene-Oligocene boundary, making inappropriate the term "Terminal Eocene Event" (Wolfe, 1978). Fossil plants do not show abrupt latest Eocene cooling, but rather long-term early Oligocene

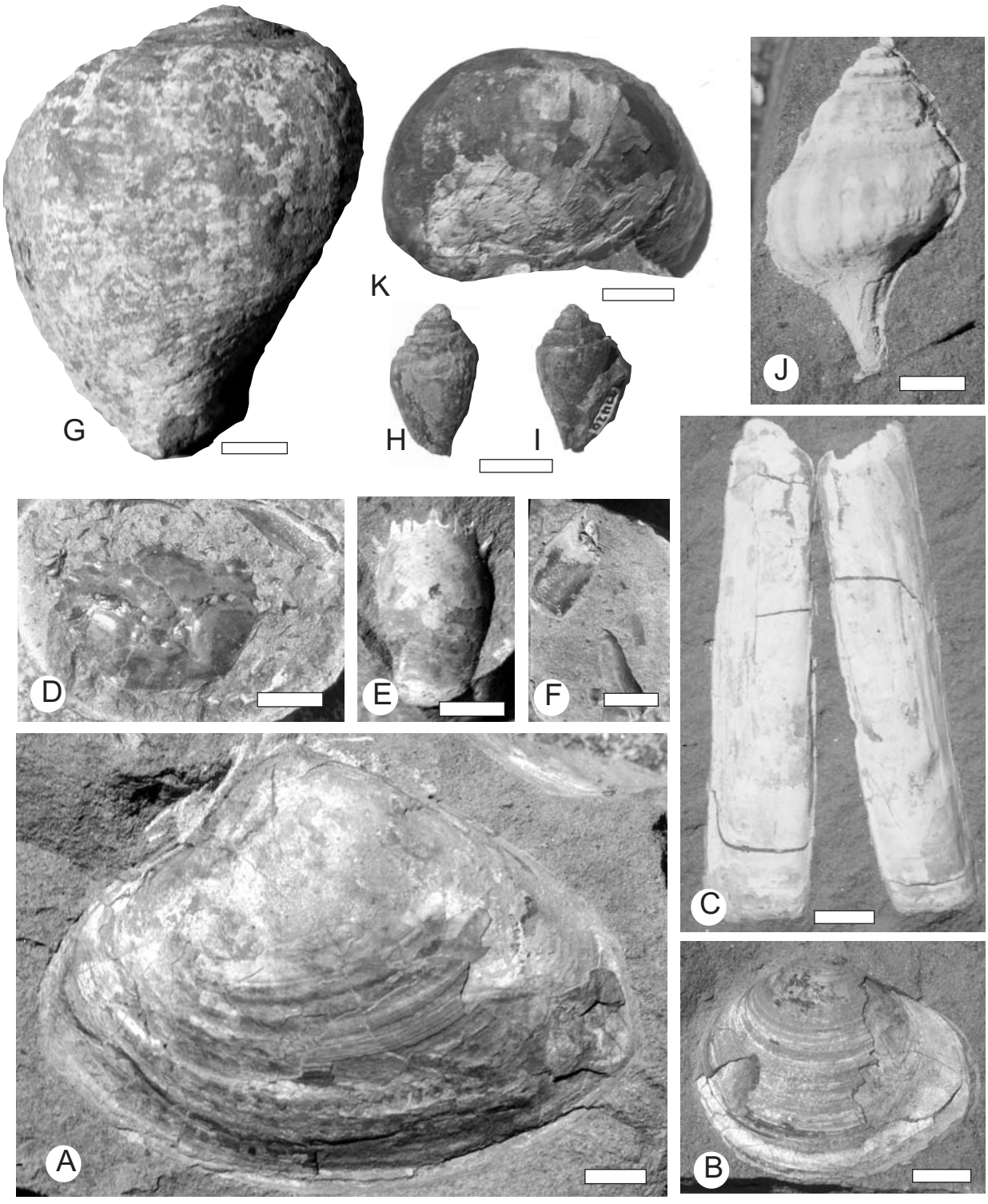

Figure 17. Selected fossil molluscs and crabs of late Eocene, Eugene fauna of lower Eugene Formation, Oregon: (A) *Spisula eugenensis* from Lillis Hall, University of Oregon (specimen numbers are for Condon Collection, University of Oregon); (B) *Macoma vancouverensis* from Lillis Hall, University of Oregon (F36231); (C) *Solena eugenensis* from Willamette Hall, University of Oregon (F36229); (D) *Megokkos magnaspina* from Glenwood (F36228A); (E) *Raninoides eugenensis* from Glenwood (F36227A); (F) *Callianassa oregonensis* from Glenwood (F36226); (G) *Ficus modesta* from College Hill (F36223); (H, I) two views of *Conus armentrouti* from 38th and University Streets, Eugene (F27420); (J) *Crepidula ungana* from Island Park, Springfield (F36224); (K) *Bruclarkia vokesi* from Willamette Hall, University of Oregon (F36225). Scale bars all 1 cm.

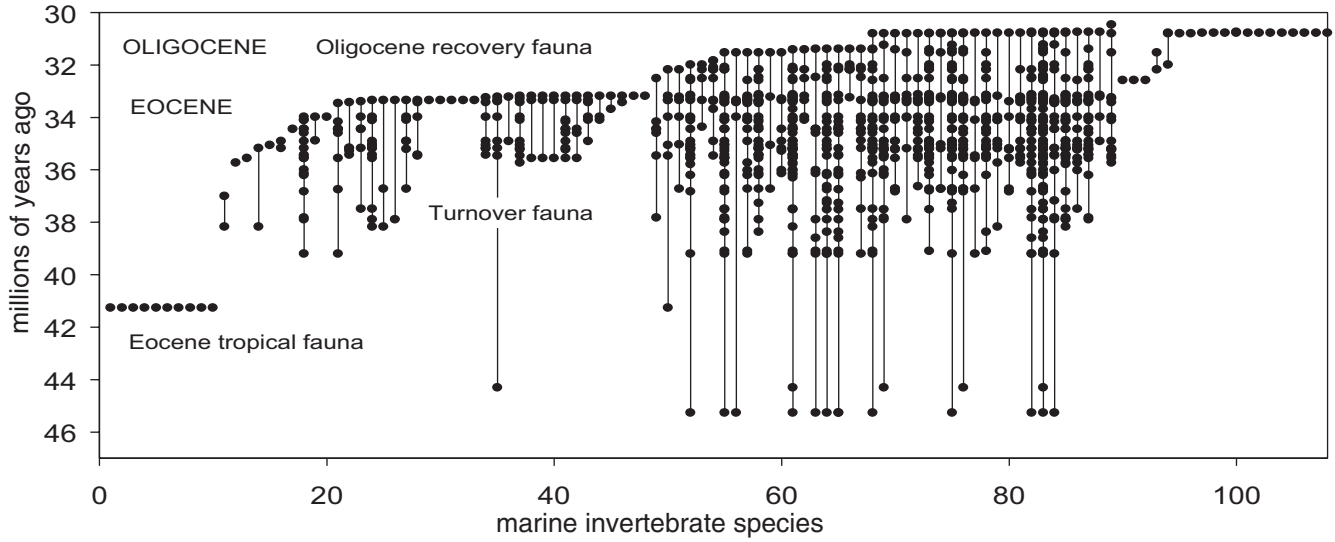

Figure 18. Stratigraphic range of marine fossils and successive marine faunas, near Eugene. 1-*Macrocallista andersoni*, 2-*Marcia bunkeri*, 3-*Pitar californiana*, 4-*Polinices nuciformis*, 5-*Solena columbiana*, 6-*Spisula rushi*, 7-*Tellina cowlitzensis*, 8-*Thracia karquinezensis*, 9-*Turritella uvasana*, 10-*Yoldia olympiana*, 11-*Kewia* sp., 12-*Conus armentrouti*, 13-*Raninoides washburnei*, 14-*Molopophorus bretzi*, 15-*Salenia schencki*, 16-*Ophiocrossota baconi*, 17-*Panopea abrupta*, 18-*Modiolus eugenensis*, 19-*Acrilla becki*, 20-*Martesia turnerae*, 21-*Yoldia tenuissima*, 22-*Priscofusus* sp, 23-*Yoldia oregona*, 24-*Ficus modesta*, 25-*Spisula pittsburgensis*, 26-*Aturia angustata*, 27-*Sinum obliquum*, 28-*Mya kusiroensis*, 29-*Callianassa* sp, 30-*Crenella* sp., 31-*Plagiolophus weaveri*, 32-*Teredo* sp., 33-*Anadara* sp., 34-*Tellina* sp., 35-*Exilia lincolnensis*, 36-*Pandora laevis*, 37-*Tellina pittsburgensis*, 38-*Megokkos macrospinus*, 39-*Raninoides eugenensis*, 40-*Raninoides fulgidus*, 41-*Acteon parvum*, 42-*Callianassa oregonensis*, 43-*Pitar* sp., 44-*Cylichnina turneri*, 45-*Palehomola gorrelli*, 46-*Zanthopsis vulgaris*, 47-*Graptocarcinus* sp., 48-*Raninoides asper*, 49-*Sanguinolaria townsendensis*, 50-*Martesia* sp., 51-*Natica* sp., 52-*Macoma vancouverensis*, 53-*Lucinoma acutilineata*, 54-*Macrocallista pittsburgensis*, 55-*Crepidula ungana*, 56-*Olequahia schenki*, 57-*Tellina lincolnensis*, 58-*Solen sicarius*, 59-*Nemocardium formosum*, 60-*Balanus* sp., 61-*Bruclarkia vokesi*, 62-*Scaphander stewarti*, 63-*Molopophorus dalli*, 64-*Pitar clarki*, 65-*Pseudocardium* sp., 66-*Epitonium condoni*, 67-*Molopophorus fishi*, 68-*Neverita thomsonae*, 69-*Dentalium lanensis*, 70-*Acila nehalemensis*, 71-*Perse lincolnensis*, 72-*Calyptraea diegoana*, 73-*Solena eugenensis*, 74-*Portlandia chehalisensis*, 75-*Parvicardium eugenense*, 76-*Nuculana washingtonensis*, 77-*Tellina aduncasana*, 78-*Thracia condoni*, 79-*Gemmula bentsoni*, 80-*Semele willamettensis*, 81-*Macrocallista* sp., 82-*Diplodonta parilis*, 83-*Spisula eugenensis*, 84-*Tellina eugenia*, 85-*Polinices washingtonensis*, 86-*Acrilla dickersoni*, 87-*Pitar dalli*, 88-*Bruclarkia columbianum*, 89-*Macoma iniquinata*, 90-*Calappa lanensis*, 91-*Persephona bigranulata*, 92-*Zanthopsis hendersonianus*, 93-*Acila shumardi*, 94-*Terebratalia transversa*, 95-*Molopophorus gabbi*, 96-*Serpulites* sp., 97-*Acmaea dickersoni*, 98-*Acmaea mitria*, 99-*Chlamys cowlitzensis*, 100-*Chlamys grunskyi*, 101-*Chlamys washburnei*, 102-*Eohemithyris alexi*, 103-*Idmonea* sp., 104-*Membranipora* sp., 105-*Mytilus snohomishensis*, 106-*Ostrea* sp., 107-*Terebratulina tejonensis*, 108-*Terria* sp. (data from Rathbun, 1926; Vokes et al., 1951; Hickman, 1969, 1980; Shroba, 1992; Schweitzer and Feldman, 2000; Burns and Mooi, 2003).

cooling (Kester, 2001; Myers, 2003), with some reversals, represented by the Sweet Home floras (Wolfe, 1971, 1992).

Comparable studies of fossil floras in central Oregon are hampered by poor age control but may indicate climatic cooling between 38 and 39 Ma (Sumner Spring flora) and also between 39 and 32.5 Ma (Nichols Spring, Canal, and Bridge Creek floras of Ashwill, 1983; Smith et al., 1998; Meyer and Manchester, 1997). Climatic cooling is evident from these floras, but they leave unconstrained the rate of paleoclimatic change.

Paleoclimatic cooling is also evident from foraminiferal, molluscan, and crustacean marine faunas of the Eugene area, with the last thermophilic elements persisting until the stratigraphic level of Glenwood (33.2 Ma), younger than the Eocene-Oligocene boundary (33.7 Ma in time scale of Berggren et al., 1995) and the abrupt oceanic isotopic shift (33.5 Ma) in deep sea cores (Zachos et al., 2001). Marine invertebrate diversity peaked during the latest Eocene (34–35 Ma), and diversity declined steadily until early Oligocene (30 Ma) marine regression from this area (Fig. 19A). Changing local sea levels, reflected in the distance southward toward Cottage Grove of marine facies (Fig. 3), also reflect a late Eocene (35 Ma) peak of warmth and marine transgression followed by cooling and retreat of sea level.

These local records can be compared with paleoclimatic records from paleosols in the John Day Fossil Beds of central Oregon (Retallack et al., 2000). The chemical composition of modern soil clay-enriched (argillic or Bt) horizons can be related to mean annual precipitation (P in mm) and mean annual temperature (T in °C) according to the following equations:

$$P = 221e^{0.0179C}$$

$$T = -18.516S + 17.278$$

where C is the molar ratio of alumina over alumina plus soda, lime, and magnesia times 100 and S is the molar ration of soda plus potash over alumina (Sheldon et al., 2002). Accuracy for precipitation ($R^2 = 0.72$, st. err. ± 185 mm) is greater than for temperature ($R^2 = 0.37$, st. err. = 4.4 °C). Mean annual precipitation can also be estimated independently from the depth to carbonate nodules (Bk horizon), in paleosols of lowland sedimentary parent materials

(Retallack, 1994, 2000; Royer, 1999), according to the following equation:

$$P = 136.6 + 6.388D – 0.01303D^2$$

where P is mean annual precipitation (mm) and D is compaction-corrected (Sheldon and Retallack, 2001) depth to Bk horizon (cm), with reasonable accuracy (R^2 = 0.8, st. dev. ± 141 mm). Paleoclimatic results from these transfer functions applied to paleosols of central Oregon are comparable to those of fossil plants and molluscs near Eugene. The late Eocene was warm and wet, with a maximum at ~35–37 Ma (Fig. 19D and E). Climatic cooling and drying was protracted with considerable fluctuation through the early Oligocene (33–28 Ma), followed by a cool and dry climate during the late Oligocene (Sheldon et al., 2002).

These paleoclimatic records from Oregon contrast with stable isotopic records from Pacific Ocean cores (Zachos et al., 2001). Shallow marine and terrestrial records of Oregon show an abrupt and short-lived paleoclimatic shift slightly after the oxygen isotopic maximum value of 3.00‰ within deep-sea foraminifera of the Pacific Ocean at 33.51 Ma (Fig. 19F), but Oregon shifts are not nearly as profound as the foraminiferal isotopic shift. The dramatic deep-sea isotopic shift is the result of at least two environmental changes, ocean-surface cooling and polar ice expansion acting in concert, which are difficult to tease apart. The carbon isotopic composition of these same foraminiferal tests also shows an abrupt positive anomaly to a maximum value of 1.64‰ at 33.47 Ma. The positive carbon anomaly reflects decreased carbon burial, which was least at 33.5 Ma and then increased carbon burial after than time. This combination of isotopic events is a paradox, because oceanic carbon oxidation adds to atmospheric CO_2 and contributes to global warming by the greenhouse effect. Yet, the oxygen isotopic positive anomaly at the same time is evidence of ice expansion and cooling at this time of minimum carbon burial at sea (Zachos et al., 2001). Furthermore, rates of accumulation of foraminifera in deep-sea cores indicate markedly increased marine productivity at this time of marine cooling and net marine carbon oxidation (Diester-Haass and Zachos, 2003). Enhanced carbon burial and productivity in continental interiors with leakage of weathered nutrients to a cooling ocean may resolve this paradox (Bestland, 2000; Retallack, 2001a).

Our diversity (Fig. 19A) and paleosol (Fig. 19D and E) data resemble the oceanic carbon isotopic record more than the oceanic oxygen isotopic record (Fig. 19F) and support modeling studies that indicate Eocene-Oligocene paleoclimatic

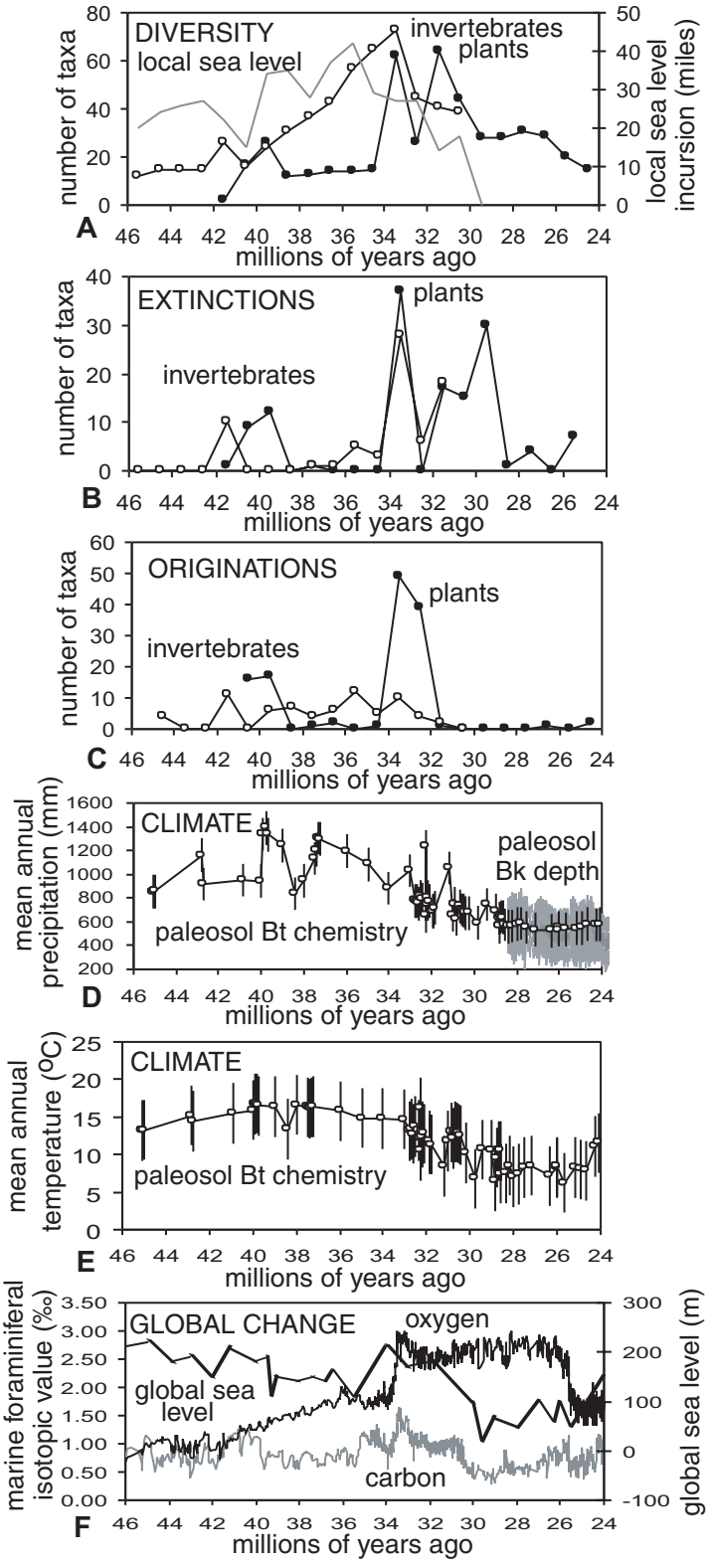

Figure 19. Species diversity (A), extinctions (B), originations (C), and local sea level (A) across the Eocene-Oligocene transition near Eugene, Oregon. Comparative paleoclimatic data from paleosols (D-E) in central Oregon are from Retallack et al. (2000) and Sheldon et al. (2002). Globally averaged oceanic isotopic data (F) is from Zachos et al. (2001) and the global sea level curve (F) is from Haq et al. (1987).

TABLE 4. PALEOCLIMATIC PARAMETERS OF FOSSIL FLORAS

Fossil flora	Geological age (Ma)	Mean annual temperature (°C)	Cold month mean temperature (°C)	Warm month mean temperature (°C)	Mean annual range of temperature (°C)	Mean annual precipitation (mm)
Sweet Home	24.7	19.7	12.1	27.3	15.2	-
Willamette	30.1	13.2	6.2	20.8	14.6	1420
Rujada	31.3	13.0	2.4	23.6	21.2	-
Goshen	33.4	19.7	6.8	25.1	18.3	3790
Comstock	39.7	22.4	7.0	26.5	19.5	3370

Note: These are the most recent estimates compiled from Wolfe (1981a, 1992, 1994), Gregory (1996), Wolfe et al. (1998), Kester (2001), Myers et al. (2002), and Myers (2003).

control by the carbon cycle (DeConto and Pollard, 2003). Oxygen isotopic curves have encouraged a view of stepwise climatic cooling and extinctions across the Eocene-Oligocene transition (Zachos et al., 2001). In contrast, the Eocene-Oligocene oceanic carbon isotopic record is more like a ramp with perturbations than a square wave or step function (Fig. 19F). A ramp with perturbation better explains our data (Figs. 19A and D–E) and other data (Poag et al., 2003) for the Eocene-Oligocene transition.

EOCENE-OLIGOCENE GLOBAL CHANGE

Fossil plants and shells from Eugene record local events such as marine regression and early western Cascades volcanism, but in addition they allow reevaluation of scenarios for Eocene-Oligocene global paleoclimatic change. Were these changes due to massive volcanism, large bolide impact, oceanic current reorganization from continental drift, or grassland ecosystem coevolution?

Tectonosedimentary regime changed little from the base of the Spencer Formation through the Eugene Formation to the top of the Fisher Formation when this area was near the Pacific Ocean coast; at times it was non-marine and at other times marine. This interval includes most of the fossil localities considered here. Earlier Eocene deep marine rocks of the Tyee Formation represent a different tectonosedimentary setting, as do dacites and basalts of the Little Butte Volcanics. Andesite and basalt flows of the Little Butte Volcanics are volumetrically much more abundant than tuffs, indicating increased volcanic edifice construction compared with the underlying Fisher Formation, but the radiometric age of the Dexter tuff indicates no long-term increase in long-term rock accumulation rate (Fig. 2). The Spencer, Eugene, Fisher, and lower Little Butte Volcanics thus constitute a record of Eocene-Oligocene events that is uncompromised by local tectonic changes. Furthermore, the record is remarkably complete because of the great thickness of these formations and active volcanism during their accumulation.

The concept of rapid environmental change is not supported by the Eocene-Oligocene boundary sequence near Eugene, which shows no "Terminal Eocene Event" (of Wolfe, 1978) nor a dramatic shift comparable to the earliest Oligocene, marine, oxygen-isotopic anomaly (Zachos et al., 2001). Instead, there is an "Oligocene deterioration" (of Wolfe, 1971, 1992), a long interval (6 Ma) of fluctuating but generally declining biodiversity that began within the early Oligocene (33.5) and reached a new equilibrium by the mid-Oligocene (29 Ma; Fig. 19A and B). Regional analysis of Pacific northwestern marine faunas (Nesbitt, 2003; Hickman, 2003) also shows a long transition from high-diversity Eocene faunas with mainly infaunal filter-feeding bivalves to low-diversity Oligocene faunas with mainly chemosynthetic and deposit-feeding bivalves. A long ramp with terminal Eocene warm and wet peaks to Oligocene cool temperate paleoclimate is also apparent from compilation of data from fossil floras throughout the Pacific Northwest (Myers, 2003). In central Oregon, paleotemperature and paleoprecipitation inferred from paleosols (Sheldon et al., 2002) show a comparable ramp of paleoclimatic deterioration (Fig. 19D and E).

There is thus no local support for the idea of the long-term paleoclimatic shift being caused by abrupt forcings such as meteorite impacts (Vonhof et al., 2000; Fawcett and Boslough, 2002) or volcanic eruptions (Kennett et al., 1985; Coulie et al., 2003). Radiometric dating of impact glass, spinels, iridium spikes, and craters indicates that impacts occurred well before the Eocene-Oligocene boundary (Hazel, 1989; Glass, 1990; Keller et al., 1983, 1987; McGhee, 2001; Poag et al., 2003). Extraterrestrial Ni-rich spinels and iridium in the stratotype section of Massignano in Italy are dated at 35.7 Ma (Pierrard et al., 1998). In deep-sea cores, iridium anomalies have been dated at 35 and 35.7 Ma, and ^{3}He anomalies at 35, 35.7, and 35.9 Ma (Farley et al., 1998). The North American tektite field is dated at 35.5 Ma (Glass et al., 1986). The 85-km-diameter Chesapeake Bay crater of the eastern United States has been dated at 35.2–35.5 ± 0.6 Ma (Poag and Aubry, 1995), the 20–22-km-diameter Toms Canyon Crater at 35.5 ± 0.6 Ma (Poag and Poppe, 1998), and the 100-km-diameter Popigai Crater of Russia at 35.7 ± 0.2 Ma (Bottomly et al., 1993). Volcanic activity in New Zealand and the surrounding ocean increased at ca. 38 Ma and continued into the Oligocene and has been argued as a cause of global cooling by atmospheric aerosol loading (Kennett et al., 1985). The Fisher Formation of the Eugene Formation shows evidence of explosive rhyodacitic volcanism of comparable age (41–30 Ma; Fig 3). Regardless of whether volcanism was continuous or episodic (McBirney, 1978), the interval 41–30 Ma was not a time of cool, dry paleoclimate but rather of wet, warm paleoclimate (Fig. 18D and E). The plateau basalts of Ethiopia and Yemen erupted largely over a period of a million years at ca. 30 Ma, with subsequent minor eruptions until 26 Ma (Coulie et al., 2003). They were thus coeval with Little Butte Volcanics near Eugene, but both postdate the Eocene-Oligocene paleoclimatic transition. Impacts and eruptions may have caused transient cooling over periods of ~100,000 yr (Vonhof et al., 2000; Fawcett and Boslough, 2002), but once the dust settled, they could not sustain long-term cooling. Impacts and eruptions are more likely to have contributed to warm paleoclimate of the late Eocene through volcanic exhalations, impact vaporization of carbonate target rock and ocean water, and oxidative destruction of plants and animals. Indeed, oxygen isotopic data from deep-sea cores (Zachos et al., 2001) and from rock exposures (Poag et al., 2003) show at least three warm paleoclimatic pulses during the late Eocene (36–33 Ma). These warm episodes can be seen as deviations from long-term paleoclimatic cooling in a manner similar to Late Devonian warm paleoclimatic excursions superimposed on a long-term cooling trend driven by carbon sequestration in evolving forests and their soils (Berner, 1997; Retallack, 1997b; McGhee, 2001).

Long-term processes such as mountain building (Raymo and Ruddiman, 1992), ocean current reorganization (Kennett, 1982), or coevolution of grasslands (Retallack, 2001a) are more likely explanations for prolonged paleoclimatic and biotic change across the Eocene-Oligocene transition. Himalayan uplift has been argued to lead Cenozoic global change, but American Cordilleran uplift also has been assigned a role (Raymo and Ruddiman, 1992). There is no local tectonic change evident from volcanic and volcaniclastic rocks of the Fisher Formation between 41 and 30 Ma, but there is much more basalt after that time, when the Eocene-Oligocene boundary transition is complete. Radiometric dating of Himalayan uplift does not indicate uplift within

the 41–30 Ma window of interest, either (Turner et al., 1993). There are also theoretical problems with estimating montane uplift from paleobotanical and sedimentological data (Molnar and England, 1990; Wolfe et al., 1998), and with the proposal that mountain uplift accelerates silicate weathering and so consumes atmospheric CO_2. In principle, soil silicates of high elevation are much less weathered than those of low elevation because of low temperatures and short growing seasons (Retallack, 2001a). In practice, low silicate weathering flux has been documented from the strontium isotopic geochemistry of Himalayan streams (Jacobson et al., 2002). Furthermore, metamorphic decarbonation and volcanism associated with mountain building contributes CO_2 to the atmosphere (Beck et al., 1998). Reduced soil and plant consumption of CO_2 at high elevations and increased CO_2 degassing from rising mountains should have warmed rather than cooled the planet, so other mechanisms are required to explain long-term global cooling.

Inception of the modern pattern of thermohaline circulation through the world ocean with the opening of ocean passages by continental drift between east Antarctica and Tasmania and between the Antarctic peninsula and South America has also been considered responsible for Eocene-Oligocene climatic cooling (Kennett, 1982; Diester-Haass and Zahn, 1996). Recent radiometric dating and core analysis in the Southern Ocean has shown that the circum-Antarctic Current was initiated by 37 Ma (Exon et al., 2002), at least 3 m.y. before the Eocene-Oligocene boundary. One could argue that a threshold width of ocean passages was needed before current volumes had a global effect, but there are other ways of viewing this effect than the thermal isolation of Antarctica. The global thermohaline conveyor is a large-scale heat pump, transporting cold saline water from the North Atlantic southward to the Southern Ocean to eventually upwell off the coast of South America, gaining warmth during westward flow through the Indonesian archipelago and then continuing around southern Africa and north into the Gulf Stream (Broecker, 1997). As a mechanism for global distribution of heat, the thermohaline conveyor is helped, not hindered, by Eocene-Oligocene northward continental drift of Australia and South America, allowing transport of increasing volumes of water through the Southern Ocean (Bice et al., 2000). Working against the warming effect of increased thermohaline conveyer flow was early Oligocene northward spread of sea ice from Antarctica (Zachos et al., 2001). Oligocene southward expansion of the cold Alaska gyre of the Oyashio current into the north Pacific Ocean (Scholl et al., 2003) introduced a variety of Asian molluscs and echinoderms into Pacific Northwestern invertebrate faunas (Hickman, 2003; Burns and Mooi, 2003) but without north Pacific ocean-current gateway reorganization. Other mechanisms are needed to explain the expansion of bipolar cold currents and sea ice.

Another gradual process for Eocene-Oligocene global change is coevolution of grasses and grazers producing grassland communities that transpired less water and had higher albedo than pre-existing woody vegetation, and had soils that weathered more rapidly and were higher in organic carbon than soils of woody vegetation (Retallack, 2001a; Jackson et al., 2002). An important new sink for carbon in atmospheric CO_2 would have been silicate weathering and organic carbon accumulation in grassland soils together with burial of carbon-rich sediment eroded from them (Retallack 1997a; Bestland, 2000). Grassland paleosols appear in the Badlands of South Dakota by ca. 33.5 Ma (Retallack, 1983, 1997a; Prothero and Whittlesey, 1998; time scale of Berggren et al., 1991), in central Oregon by ca. 30 Ma (Retallack et al., 2000), and in other parts of the world at comparable times (Retallack, 1992). Grass phytoliths (Meehan, 1994; Strömberg, 2002) and pollen (Morley and Richards, 1993; Jacobs et al., 1999) rise in abundance at the same times. Fossil mammals show some adaptations, such as increased cursoriality (Bakker, 1983) and more fully lophed teeth (Janis, 1997), to these changes at 33.5 Ma. However, mammalian hypsodonty expected from the coarse phytolith-rich nature of grassy graze increased only slightly at 33.5 Ma, with greater hypsodonty increases at 28 and 19 Ma (Janis et al., 2002). Chemical analysis of paleosols reveals increased rates of chemical weathering across the Eocene-Oligocene transition in central Oregon (Bestland, 2000). Such increased weathering and productivity of rangelands would also have delivered more nutrients to fuel productivity increases in the ocean, which are observed despite concomitant cooling of the ocean (Diester-Haass and Zahn, 1996; Diester-Haass and Zachos, 2003). Global drawdown of CO_2 over the Eocene-Oligocene transition is indicated by stomatal index increases in fossil *Ginkgo* leaves from Sakhalin, Primorie, and Japan (Retallack, 2001b, 2002). The increased distribution of grasslands to an area sufficient to affect global climate is a threshold feature of this model, comparable with thresholds of Southern Ocean spreading. Bunch grasslands at this time were largely in dry continental interiors (Retallack, 2001a), remote from coastal regions such as Eugene. Nevertheless, changes in Oregon's coastal floras detailed here well match paleoclimatic changes inferred from central Oregon's fossil floras (Meyer and Manchester, 1997; Myers, 2003) and soils (Retallack et al., 2000), including increased abundance of wind-pollinated angiosperms and swampland dominance by taxodiaceous conifers rather than angiosperms (Wolfe, 1992). Once the post-apocalyptic greenhouses of multiple late Eocene impacts had been assimilated by the global carbon cycle, the full force of grasslands as a newly evolved carbon sink became apparent at 33.5 Ma, with continuing adjustments to grassland expansion until 29 Ma. The Eocene-Oligocene boundary has long been recognized as a time of floristic modernization in North America. Whether or not grasslands were a cause or consequence of global change, the Eocene-Oligocene transition heralded the advent of grassland ecosystems.

ACKNOWLEDGMENTS

Retallack thanks Bretagne Hygelund, Julie Eurek, Douglas Ridenour, A. Edwards, Lawrence Palmer, Robert Lenegan, Robert Schutt, P. Collinson, and Christopher Grundner-Culeman for assistance with sedimentary petrology, and Nathan Sheldon for manuscript review. Prothero thanks Clio Bitboul, Linda Donohoo, Elizabeth Draus, Elana Goer, Karina Hankins, Jonathan Hoffman, Teresa Le Velle, and Elizabeth Sanger for help with paleomagnetic sampling, and Joe Kirschvink for access to the Caltech paleomagnetics laboratory. Duncan thanks John Huard for laboratory assistance with radiometric dating. Prothero was supported by NSF grants EAR97–06046, EAR98–05071, and EAR00–00174, and by a grant from the Donors of the Petroleum Research Fund of the American Chemical Society.

REFERENCES CITED

Addicott, W.O., 1981, Significance of pectinids in Tertiary biochronology of the Pacific Northwest, *in* Armentrout, J.M., ed., Pacific Northwest Cenozoic biostratigraphy: Geological Society of America Special Paper 184, p. 17–37.

Anderson, R.W., 1963, Geology of the northwest quarter of the Brownsville Quadrangle, Oregon [M.S. thesis]: Eugene, University of Oregon, 62 p.

Armentrout, J.M., 1981, Correlation and ages of Cenozoic chronostratigraphic units in Oregon and Washington, *in* Armentrout, J.M., ed., Pacific Northwest Cenozoic biostratigraphy: Geological Society of America Special Paper 184, p. 137–147.

Ashwill, M., 1983, Seven fossil floras in the rain shadow of the Cascade Mountains, Oregon: Oregon Geology, v. 45, p. 107–111.

Ashwill, W.R., 1951, The geology of the Winberry Creek area, Lane County, Oregon [M.S. thesis]: Eugene, University of Oregon, 63 p.

Axelrod, D.I., 1992, Climatic pulses, a major factor in legume evolution, *in* Herendeen, P.S., and Dilcher, D.L., eds., Advances in legume systematics: Kew, Royal Botanical Gardens, p. 259–279.

Bakker, R.T., 1983, The deer flees: The wolf pursues: Incongruencies in predator-prey coevolution, *in* Futuyma, D.J., and Slatkin, M., eds., Coevolution: Sunderland: Massachusetts, Sinauer, p. 350–382.

Bales, W.E., 1951, Geology of the lower Brice Creek area, Lane County, Oregon [M.S. thesis]: Eugene, University of Oregon, 55 p.

Baldwin, E.M., 1981, Geology of Oregon: Dubuque, Kendall/Hunt, 170 p.

Beck, R.A., Sinha, A., Burbank, D.W., Sercombe, W.J., and Khan, A.M., 1998, Climatic, oceanographic and isotopic consequences of the Paleocene India-Asia

collision, *in* Aubry, M.-P., Lucas, S., and Berggren, W.A., eds., Late Paleocene–early Eocene climatic events in the marine and terrestrial records: New York, Columbia University Press, p. 103–117.

Berggren, W.A., Kent, D.V., Swisher, C.C., and Aubry, M.P., 1995, A revised Cenozoic geochronology and chronostratigraphy, *in* Berggren, W.A., Kent, D.V., Aubry, M.P., and Hardenbol, J., eds., Geochronology, time scales, and global stratigraphic correlation: Society for Sedimentary Geology (SEPM) Special Publication 54, p. 129–212.

Berner, R.A., 1997, The rise of land plants and their effect on weathering and atmospheric CO_2: Science, v. 276, p. 543–546.

Bestland, E.A., 1987, Volcanic stratigraphy of the Oligocene Colestin Formation in the Siskiyou Pass area of southern Oregon: Oregon Geology, v. 49, p. 79–86.

Bestland, E.A., 2000, Weathering flux and CO_2 consumption determined from paleosol sequences across the Eocene-Oligocene transition: Palaeogeography, Palaeoclimatology, Palaeoecology, v. 156, p. 301–326.

Bestland, E.A., Hammond, P.E., Blackwell, D.L.S., Kays, M.A., Retallack, G.J., and Stimac, J., 1999, Geologic framework of the Clarno Unit of the John Day Fossil Beds National Monument, central Oregon: Oregon Geology, v. 61, p. 3–19.

Bice, K.L., Scotese, C.R., Seidev, D., and Barron, E.J., 2000, Quantifying the role of geographic change in Cenozoic ocean heat transport: Palaeogeography, Palaeoclimatology, Palaeoecology, v. 161, p. 295–310.

Bottomly, R.J., York, D., and Grieve, R.A.F., 1993, Age of the Popigai impact event using the $^{40}Ar/^{39}Ar$ method: Lunar and Planetary Science Conference Abstracts v. 24, p. 161.

Boucot, A.J., 1990, Evolution and paleobiology of behavior and coevolution: Amsterdam, Elsevier, 723 p.

Bristow, M.M., 1959, The geology of the northwestern third of the Marcola Quadrangle [M.S. thesis]: Eugene, University of Oregon, 70 p.

Broecker, W.S., 1997, Thermohaline circulation, the Achilles heel of our current climate system: Will man-made CO_2 upset the current balance?: Science, v. 278, p. 1582–1588.

Brown, R.W., 1950, An Oligocene evergreen cherry from Oregon: Washington Academy of Science Journal, v. 40, p. 321–324.

Brown, R.W., 1959, A bat and some plants from the upper Oligocene of Oregon: Journal of Paleontology, v. 33, p. 125–129.

Burns, C., and Mooi, R., 2003, An overview of Eocene-Oligocene echinoderm faunas of the Pacific Northwest, *in* Prothero, D.R., Ivany, L.C., and Nesbitt, E.A., eds., From Greenhouse to Icehouse: The marine Eocene Oligocene transition: New York, Columbia University Press, p. 397–416.

Cande, S.C., and Kent, D.V., 1995, Revised calibration of the geomagnetic polarity timescale for the Late Cretaceous and Cenozoic: Journal of Geophysical Research, v. 100, p. 6093–6095.

Chaney, R.W., 1948, The ancient forests of Oregon: Eugene, Oregon State System of Higher Education, 56 p.

Chaney, R.W., and Sanborn, E.I., 1933, The Goshen flora of central Oregon: Carnegie Institution of Washington Publication, v. 439, 237 p.

Clymer, A.K., Bice, D.M., and Montanari, A., 1996, Shocked quartz from the late Eocene: Impact evidence from Massignano, Italy: Geology, v. 24, p. 483–486.

Coulie, E., Quidelleur, X, Gillet, P.Y., Courtillot, V., Lefevre, J.C., and Chiesa, S., 2003, Comparative K-Ar and Ar/Ar dating of Ethiopian and Yemenite Oligocene volcanism: Implications for timing and duration of the Ethiopian Traps: Earth and Planetary Science Letters, v. 200, p. 477–292.

Crane, P.R., and Stockey, R.A., 1985, Growth and reproductive biology of *Joffrea speirsii* gen. et sp. nov., a *Cercidiphyllum*-like plant fossils from the late Paleocene of Alberta, Canada: Canadian Journal of Botany, v. 63, p. 340–364.

Dalrymple, G.B., 1979, Critical tables for conversion of K-Ar ages from old to new constants: Geology, v. 7, p. 558–560.

DeConto, R.M., and Pollard, D., 2003, Rapid Cenozoic glaciation of Antarctica induced by declining atmospheric CO_2: Nature, v. 421, p. 245–248.

Demarest, H.H., 1983, Error analysis for the determination of tectonic rotation from paleomagnetic data: Journal of Geophysical Research, v. 88, p. 4321–4328.

Diehl, J.F., Beck, M.E., Beske-Diehle, S., Jacobson, D., and Hearn, B.C., 1983, Paleomagnetism of the Late Cretaceous–early Tertiary north central Montana alkalic province: Journal of Geophysical Research, v. 88, p. 10,593–10,609.

Diester-Haass, L., and Zahn, R., 1996, The Eocene-Oligocene transition in the Southern Ocean: History of water masses, circulation and biological productivity inferred from high resolution records of stable isotopes and benthic foraminiferal abundances (ODP site 689): Geology, v. 24, p. 16–20.

Diester-Haass, L., and Zachos, J., 2003, The Eocene-Oligocene transition in the equatorial Atlantic (ODP site 925): Paleoproductivity increase and positive $\delta^{13}C$ excursion, *in* Prothero, D.R., Ivany, L.C., and Nesbitt, E.A., eds., From Greenhouse to Icehouse: The marine Eocene Oligocene transition: New York, Columbia University Press, p. 397–426.

Dolph, G.E., 1979, Variation in leaf margin with respect to climate in Costa Rica: Torrey Botanical Club Bulletin, v. 106, p. 104–109.

Dolph, G.E., and Dilcher, D.L., 1979, Foliar physiognomy as an aid in determining paleoclimate: Palaeontographica, v. 170B, p. 151–172.

Doyle, J.A., Shorn, H.E., Tiffney, B.H., and Upchurch, G.R., eds., 1988, The La Porte flora—Early Oligocene of north central California: Field Guidebook for the Paleobotanical Section of the Botanical Society of America Meeting, Davis, 81 p.

Duncan, R.A., 2002, A time frame for construction of the Kerguelen Plateau and Broken Ridge: Journal of Petrology, v. 43, p. 163–166.

Durham, J.W., 1944, Megafaunal zones of the Oligocene of northwestern Washington: University of California Department of Geological Sciences Bulletin, v. 27, p. 101–211.

Eubanks, W., 1962, The fossil flora of Thomas Creek: The Ore Bin, v. 24, p. 26–29.

Evanoff, E., Prothero, D.R., and Lander, R.H., 1992, Eocene–Oligocene climatic change in North America: The White River Formation near Douglas, east-central Wyoming, *in* Prothero, D.R., and Berggren, W.A., eds., Eocene–Oligocene climatic and biotic evolution: Princeton, Princeton University Press, p. 116–130.

Evernden, J.F., and James, G.T., 1964, Potassium-argon dates of the Tertiary floras of North America: American Journal of Science, v. 262, p. 945–974.

Exon, N., et al., 2002, Drilling reveals climatic consequences of Tasmanian Gateway opening: Eos (Transactions, American Geophysical Union) v. 83, p. 253–259.

Farley, K.A., Montanari, A., Shoemaker, E.M., and Shoemaker, C.S., 1998, Geochemical evidence for a comet shower in the late Eocene: Science, v. 280, p. 1250–1259.

Fawcett, P.J., and Boslough, M.B.E., 2002, Climate effects of an impact-induced equatorial debris ring: Journal of Geophysical Research, v. 107, p. 10,129–10,146.

Feibelkorn, R.B., Walker, G.W., MacLeod, N.S., McKee, E.H., and Smith, J.G., 1982, Index to K-Ar age determinations for the state of Oregon: Isochron West, v. 37, p. 3–60.

Fischer, J.F., 1976, K-Ar dating from the Stevens Ridge Formation, Cascade Range, central Washington: Isochron West, v. 16, p. 31.

Fisher, R.A., 1953, Dispersion on a sphere: Royal Society of London Proceedings, v. A217, p. 295–305.

Fisher, R.V., 1966, Geology of a Miocene ignimbrite layer, John Day region, eastern Oregon: Publications in Geological Sciences, University of California, v. 67, 59 p.

Fraser, F.C., 1955, A odonate fossil wing from the Oligocene of Oregon: Psyche, v. 62, p. 42–44.

Fremd, T., Bestland, E.A., and Retallack, G.J., 1994, John Day Basin field trip guide and road log for the Society of Vertebrate Paleontology Field Trip: Seattle, Northwest Interpretive Association, 90 p.

Givnish, T.J., 1987, Comparative studies of leaf form: Assessing the relative size of selective pressures and phylogenetic constraints: New Phytologist, v. 106, p. 131–160.

Glass, B.P., 1990, Chronostratigraphy of upper Eocene microspherules: Comment: Palaios, v. 5, p. 387–389.

Glass, B.P., and Zwart, M.J., 1979, North American microtektites in Deep Sea Drilling Project cores from the Carribean Sea and Gulf of Mexico: Geological Society of America Bulletin, v. 90, p. 595–602.

Glass, B.P., Hall, C.M., and York, D., 1986, $^{40}Ar/^{39}Ar$ laser probe dating of North American tektite fragments from Barbados and age of the Eocene-Oligocene boundary: Chemical Geology, v. 59, p. 181–186.

Graven, E.P., 1990, Structure and tectonics of the southern Willamette Valley, Oregon [M.S. thesis]: Corvallis, Oregon State University, 119 p.

Greenwood, D.R., 1992, Taphonomic constraints on foliar physiognomic interpretations of Late Cretaceous and Tertiary paleoclimates: Reviews of Palaeobotany and Palynology, v. 71, p. 149–190.

Gregory, I., 1968, The fossil woods near Holley in the Sweet Home Petrified Forest, Linn County, Oregon: The Ore Bin, v. 30, p. 57–76

Gregory, K.M., 1994, Palaeoclimate and palaeoelevation of the 35 Ma Florissant flora, Front Range, Colorado: Palaeoclimates, v. 1, p. 23–57.

Gregory, K.M., 1996, Are paleoclimatic estimates biased by foliar physiognomic responses to increased atmospheric CO_2?: Palaeogeography, Palaeoclimatology, Palaeoecology, v. 124, p. 39–51.

Gurevitch, J., 1988, Variation in leaf dissection and leaf energy budgets among populations of *Achillea* from an altitudinal gradient: American Journal of Botany, v. 75, p. 1298–1306.

Hagee, V.L., and Olson, P., 1989, An analysis of paleomagnetic secular variation in the Holocene: Physics of Earth and Planetary Interiors, v. 56, p. 266–284.

Haq, B.U., Hardenbol, J., and Vail, P.R., 1987, Chronology of fluctuating sea levels since the Triassic (250 million years ago to present): Science, v. 235, p. 1156–1167.

Hauck, S.M., 1962, Geology of the southwest quarter of the Brownsville Quadrangle, Oregon [M.S. thesis]: Eugene, University of Oregon, 82 p.

Hazel, J.E., 1989, Chronostratigraphy of upper Eocene microspherules: Palaios, v. 4, p. 318–329.

Hausen, D.M., 1951, Welded tuff along the Row River, western Oregon [M.S. thesis]: Eugene, University of Oregon, 98 p.

Hertlein, L.G., and Grant, U.S., 1944, The Cenozoic Brachiopoda of western North America: University of California Publications in Mathematics and Physical Sciences, v. 3, 236 p.

Hickman, C.J.S., 1969, The Oligocene marine molluscan fauna of the Eugene Formation in Oregon: University of Oregon Museum of Natural History Bulletin, v. 16, 112 p.

Hickman, C.J.S., 1980, Paleogene marine gastropods of the Keasey Formation in Oregon: Bulletins of American Paleontology, v. 78, 112 p.

Hickman, C.J.S., 2003, Evidence for abrupt Eocene–Oligocene molluscan faunal change in the Pacific Northwest, *in* Prothero, D.R., Ivany, L.C., and Nesbitt, E.A., eds., From Greenhouse to Icehouse: The marine Eocene Oligocene transition: New York, Columbia University Press, p. 71–87.

Hladky, F.R., Wiley, T.J., and Duncan, R.A., 1992, Volcanic stratigraphy and new whole-rock K-Ar ages of western Cascades rocks in southern Oregon: Geological Society of America Abstracts, v. 24, no. 5, p. 33.

Hoover, L., 1963, Geology of the Anlauf and Drain Quadrangles, Douglas and Lane Counties, Oregon: U.S. Geological Survey Bulletin, v. 1122D, p. D1–D62.

Hutchison, J.H., 1992, Western North American reptile and amphibian record across the Eocene/Oligocene boundary and its climatic implications, *in* Prothero, D.R., and Berggren, W.A., eds., Eocene-Oligocene climatic and biotic evolution: Princeton, Princeton University Press, p. 451–463.

Jackson, R.B., Banner, J.L., Jobbágy, E.G., Pockman, W.T., and Wall, D.H., 2002, Ecosystem carbon loss with woody plant invasion of grasslands: Nature, v. 418, p. 623–626.

Jacobs, B.F., Kingston, J.D., and Jacobs, L.L., 1999, The origin of grass-dominated ecosystems: Missouri Botanical Garden Annals, v. 86, p. 590–643.

Jacobson, A.D., Blum, J.D., and Walter, L.M., 2002, Reconciling the elemental and Sr isotopic composition of Himalayan weathering fluxes: Insights from the carbonate geochemsitry of stream waters: Geochimica et Cosmochimica Acta, v. 66, p. 4317–3429.

Janis, C.M., 1997, Ungulate teeth, diets and climatic changes at the Eocene/Oligocene boundary: Zoology, v. 100, p. 203–220.

Janis, C.M., Damuth, J., and Theodor, J.M., 2002, The origins and evolution of the North American grassland biome:

The story from the hoofed mammals: Palaeogeography, Palaeoclimatology, Palaeoecology, v. 177, p. 183–198.
Jefferson, T.H., 1982, Fossil forests from the Lower Cretaceous of Alexander Island, Antarctica: Palaeontology, v. 25, p. 681–708.
Keller, G., d'Hondt, S.L., and Vallier, T.L., 1983, Multiple microtektite horizons in upper Eocene marine sediments: No evidence for mass extinction: Science, v. 224, p. 309–310.
Keller, G., D'Hondt, S.L., Orth, C.J., Gilmore, J.S., Oliver, P.Q., Shoemaker, E.M., and Molina, E., 1987, Late Eocene impact microspherules: Stratigraphy, age and geochemistry: Meteoritics, v. 22, p. 25–60.
Kennett, J.P., 1982, Marine geology: Englewood Cliffs, New Jersey, Prentice-Hall, 813 p.
Kennett, J.P., von der Borch, C., Baker, P.A., Barton, C.E., Boersma, A., Cauler, J.P., Dudley, W.C., Gardner, J.V., Jenkins, P.G., Lohman, W.H., Martini, E., Merrill, R.B., Morin, R., Nelson, C.S., Robert, C., Srinivasam, M.S., Stein, R., Takeuchi, A., and Murphy, M.A., 1985, Paleotectonic implications of increased late Eocene-early Oligocene volcanism from South Pacific DSDP sites: Nature, v. 316, p. 507–511.
Kerp, H., and Krings, M., 1999, Light microscopy of cuticles, *in* Jones, T.P., and Rowe, N.P., eds., Fossil plants and spores: Modern techniques: London, Geological Society, p. 52–565.
Kester, P.R., 2001, Paleoclimatic interpretation from the early Oligocene Willamette flora, Eugene [M.S. thesis]: Seattle, University of Washington, 146 p.
Kirschvink, J.L., 1980, The least-squares line and plane and the analysis of paleomagnetic data: Examples from Siberia and Morocco: Geophysical Journal of the Royal Astronomical Society, v. 62, p. 699–718.
Klucking, E., 1964, An Oligocene flora from the western Cascades [Ph.D. thesis]: Berkeley, University of California, 241 p.
Koppers, A.A.P., 2002, ArArCALC; software for $^{40}Ar/^{39}Ar$ age calculations: Computers and Geosciences, v. 28, p. 605–619.
Lakhanpal, R.N., 1958, The Rujada flora of west central Oregon: University of California, Publications in Geological Sciences, v. 35, p. 1–66.
LaMotte, R.S., 1952, Catalogue of the Cenozoic plants of North America through 1950: Boulder, Colorado, Geological Society of America Memoir 51, 381 p.
Langenhorst, F., and Clymer, A.K., 1996, Characteristics of shocked quartz in late Eocene impact ejecta from Massignano (Ancona, Italy): Clues to shock conditions and source crater: Geology, v. 24, p. 487–490.
Laursen, J.M., and Hammond, P.E., 1974, Summary of radiometric ages of Oregon and Washington rocks through June 1972: Isochron West, v. 9, p. 1–32.
Lewis, R.Q., 1951, The geology of the southern Coburg Hills, including the Springfield-Goshen area [M.S. thesis]: Eugene, University of Oregon, 58 p.
Linder, R.A., Durham, J.W., and Orr, W.N., 1988, New late Oligocene echinoids from the central western Cascades of Oregon: Journal of Paleontology, v. 62, p. 945–958.
Lowry, W.D., 1947, Foundry sand produced near Eugene, Oregon: American Institute of Mining and Metallurgical Engineering Technical Publication 2058, p. 1–10.
Lux, D.R., 1981, K-Ar and $^{40}Ar/^{39}Ar$ ages of mid-Tertiary volcanic rocks from the western Cascade Range, Oregon: Isochron West, v. 33, p. 27–32.
MacPherson, B.A., 1953, The geology of the Halsey Quadrangle, Oregon [M.S. thesis]: Eugene, University of Oregon, 64 p.
Maddox, T., 1965, Geology of the southern third of the Marcola Quadrangle, Oregon [M.S. thesis]: Eugene, University of Oregon, 78 p.
Manchester, S.R., 1986, Vegetative and reproductive morphology of an extinct plane tree (Platanaceae) from the Eocene of western North America: Botanical Gazette, v. 147, p. 200–226.
Manchester, S.R., 1992, Flowers, fruits, and pollen of *Florissantia*, an extinct Malvalean genus from the Eocene and Oligocene of western North America: American Journal of Botany, v. 79, p. 996–1008.
McBirney, A.R., 1978, Volcanic evolution of the Cascade Range: Annual Reviews of Earth and Planetary Sciences, v. 6, p. 437–456.
McDougall, C., and Harrison, T.M., 1999, Geochronology and thermochronology by $^{40}Ar/^{39}Ar$ method, 2nd edition: New York, Oxford University Press, 269 p.
McDougall, K., 1980, Paleoecological evaluation of late Eocene biostratigraphic zonations of the Pacific coast of North America: Paleontological Monograph, Journal of Paleontology, v. 54, v. 2, p. 1–75.
McFadden, P.L., and McElhinney, M.W., 1980, Classification of the reversal test in paleomagnetism: Geophysical Journal International, v. 103, p. 725–729.
McGhee, G.R., 2001, The "multiple impacts" hypothesis for mass extinction: A comparison of the Late Devonian and late Eocene: Palaeogeography, Palaeoclimatology, Palaeoecology, v. 176, p. 47–58.
McKillip, C.J., 1992, Paleoenvironvironment and biostratigraphy of the Eugene Formation, near Salem, Oregon [M.S. thesis]: Eugene, University of Oregon, 108 p.
Mears, K.A., 1989, Petrography and provenance of the Eugene Formation, Lane County, Oregon [M.S. thesis]: Eugene, University of Oregon, 126 p.
Meehan, T.J., 1994, Sediment analysis of the middle Whitney Member: Climatic implications of the upper Oligocene of Nebraska, *in* Dort, W., ed., TERQUA Symposium Series: Lincoln, Nebraska, University of Nebraska Press, v. 2, p. 57–87.
Meyer, H., 1973, The Oligocene Lyons flora of northwestern Oregon: The Ore Bin, v. 35, p. 37–51.
Meyer, H.W., and Manchester, S.R., 1997, Revision of the Oligocene Bridge Creek floras of Oregon: University of California, Publications in Geological Sciences, v. 141, 195 p.
Miller, P.R., and Orr, W.N., 1987, The Scotts Mills Formation: Mid-Tertiary geologic history and paleogeography of the central western Cascade Range, Oregon: Oregon Geology, v. 48, p. 139–151.
Millhollen, G.L., 1991, Welded tuffs of the Winberry Creek area, central Oregon Cascade Range: Oregon Geology, v. 53, p. 89–91.
Molnar, P., and England, P., 1990, Late Cenozoic uplift of mountain ranges and global cooling: Chicken or egg?: Nature, v. 240, p. 29–34.
Montanari, A., Asaro, F., Michel, H.V., and Kennett, J.P., 1993, Iridium anomalies of late Eocene age at Massignano (Italy), and ODP site 689B (Maud Rise, Antarctica): Palaios, v. 8, p. 420–437.
Morley, R.J., and Richards, K., 1993, Gramineae cuticle, key indicator of late Cenozoic climatic change in the Niger River Delta: Review of Palaeobotany and Palynology, v. 77, p. 119–127.
Murray, R.B., 1994, Geology and mineral resources of the Richter Mountain 7.5 minute Quadrangle, Douglas and Jackson Counties, Oregon [M.S. thesis]: Eugene, University of Oregon, 239 p.
Myers, J.A., 2003, Terrestrial Eocene-Oligocene vegetation and climate of the Pacific Northwest, *in* Prothero, D.R., Ivany, L.C., and Nesbitt, E., eds., From Greenhouse to Icehouse: The Marine Eocene-Oligocene Transition: New York, Columbia University Press, p. 171–185.
Myers, J.A., Kester, P.R., and Retallack, G.J., 2002, Paleobotanical record of Eocene-Oligocene climate and vegetation change near Eugene, Oregon, *in* Moore, G.W., ed., Field guide to geological processes in Cascadia: Oregon Department of Geology and Mineral Industries Special Paper 36, p. 15–54.
Nesbitt, E.A., 2003, Changes in shallow-marine faunas from the northweastern Pacific margin ascross the Eocene-Oligocene boundary, *in* Prothero, D.R., Ivany, L.C., and Nesbitt, E., eds., From Greenhouse to Icehouse: The Marine Eocene-Oligocene Transition: New York, Columbia University Press, p. 57–61.
Opdyke, N.D., Lindsay, E.H., Johnson, N.M., and Downs, T., 1977, The paleomagnetism and magnetic polarity stratigraphy of the mammal-bearing section of Anza-Borrego State Park, California: Quaternary Research, v. 17, p. 316–329.
Oyen, L.W., and Portell, R.W., 2001, Diversity patterns and biostratigraphy of Cenozoic echinoderms from Florida: Palaeogeography, Palaeoclimatology, Palaeoecology, v. 166, p. 193–218.
Peck, D.L., Griggs, A.L., Schlicker, H.G., Wells, F.G., and Dole, H.M., 1964, Geology of the central and northern parts of the western Cascade Range in Oregon: U.S. Geological Survey Professional Paper 449, 56 p.
Pierrard, O., Robin, E., Rocchia, R, and Montanari, A., 1998, Extraterrestrial Ni-rich spinel in upper Eocene sediments from Massignano, Italy: Geology, v. 86, p. 307–310.
Pluhar, C., Kirschvink, J.L., and Adams, R.W., 1991, Magnetostratigraphy and clockwise rotation of the Plio-Pleistocene Mojave River Formation, central Mojave Desert, California: San Bernardino Association Quarterly, v. 38, no. 2, p. 31–42.
Poag, C.W., and Aubry, M.P., 1995, Upper Eocene impactites of the U.S., east coast: Depositional origins, biostratigraphic framework, and correlation: Palaios, v. 10, p. 16–43.
Poag, C.W., and Poppe, L.J., 1998, The Toms Canyon structure, New Jersey, outer continental shelf: A possible late Eocene impact crater: Marine Geology, v. 145, p. 23–60.
Poag, C.W., Powars, D.S., Poppe, L.J., and Mixon, R.B., 1994, Meteoroid mayhem in Ole Virginny: Source of the North American textite strewn field: Geology, v. 22, p. 691–694.
Poag, C.W., Mankinen, E., and Norris, P., 2003, Late Eocene impacts: Geologic record, correlation and paleoenvironmental consequences, *in* Prothero, D.R., Ivany, L.C., and Nesbitt, E., eds., From Greenhouse to Icehouse: The Marine Eocene-Oligocene Transition: New York, Columbia University Press, p. 495–510.
Potbury, S.S., 1935, The La Porte flora of Plumas County, California: Washington, D.C., Publications of the Carnegie Institution of Washington, v. 465, p. 1–28.
Prothero, D.R., 1994a, The Eocene-Oligocene Transition: Paradise Lost: New York, Columbia University Press, 281 p.
Prothero, D.R., 1994b, The late Eocene-Oligocene extinctions: Annual Reviews of Earth and Planetary Sciences, v. 22, p. 145–165.
Prothero, D.R., 2001, Chronostratigraphic calibration of the Pacific Coast Cenozoic: A summary, *in* Prothero, D.R., ed., Magnetic stratigraphy of the Pacific Coast Cenozoic: Fullerton, Pacific Section SEPM (Society for Sedimentary Geology), no. 91, p. 377–391.
Prothero, D.R., and Donohoo, L.L., 2001a, Magnetic stratigraphy and tectonic rotation of the middle Eocene Coaledo Formation, southwestern Oregon: Geophysical Journal International, v. 145, p. 1–15.
Prothero, D.R., and Donohoo, L.L., 2001b, Magnetic stratigraphy of the lower Oligocene Tunnel Point Formation, Coos Bay, southwestern Oregon, *in* Prothero, D.R., ed., Magnetic stratigraphy of the Pacific Coast Cenozoic: Fullerton, Pacific Section SEPM (Society for Sedimentary Geology), no. 91, p. 195–200.
Prothero, D.R., and Hankins, K.G., 2000, Magnetic stratigraphy and tectonic rotation of the upper Eocene-lower Oligocene Keasey Formation, northwest Oregon: Journal of Geophysical Research, v. 105, p. 16,473–16,480.
Prothero, D.R., and Hankins, K.G., 2001, Magnetic stratigraphy and tectonic rotation of the lower Oligocene Pittsburg Bluff Formation, Columbia County, Oregon, *in* Prothero, D.R., ed., Magnetic stratigraphy of the Pacific Coast Cenozoic: Fullerton, Pacific Section SEPM (Society for Sedimentary Geology), no. 91, p. 201–209.
Prothero, D.R., and Whittlesey, K.E., 1998, Magnetic stratigraphy and biostratigraphy of the Orellan and Whitneyan land-mammal "ages" in the White River Group, *in* Terry, D.O., LaGarry, H.E., and Hunt, R.M., eds., Depositional environments, lithostratigraphy and biostratigraphy of the White River and Arikaree Groups (late Eocene to early Miocene), North America: Geological Society of America Special Paper 325, p. 39–61.
Prothero, D.R., Bitboul, C., Moore, G.W., and Niem, A.R., 2001a, Magnetic stratigraphy and tectonic rotation of the Oligocene Alsea, Yaquina, and Nye Formations, Lincoln County, Oregon, *in* Prothero, D.R., ed., Magnetic stratigraphy of the Pacific coast Cenozoic: Fullerton, Pacific Section SEPM (Society for Sedimentary Geology), no. 91, p. 184–194.
Prothero, D.R., Sanger, E, Nesbitt, E., Niem, A., and Kliebaker, D., 2001b, Magnetic stratigraphy and tectonic rotation of the upper middle Eocene Cowlitz and Hamlet Formations, western Oregon and Washington, *in* Prothero, D.R., ed., Magnetic stratigraphy of the Pacific Coast Cenozoic: Fullerton, Pacific Section SEPM (Society for Sedimentary Geology), no. 91, p. 75–95.
Rathbun, M.J., 1926, The fossil stalk-eyed crustacea of the Pacific slope of North America: U.S. National Museum Bulletin, v. 138, 155 p.
Raymo, M.E., and Ruddiman, M.F., 1992, Tectonic forcing of late Cenozoic climate: Nature, v. 359, p. 117–122.

Renne, P.R., Deino, A.L., Walter, R.C., Turrin, B.D., Swisher, C.C., Becker, T.A., Curtis, G.H., Sharp, W.D., and Jaouni, A.R., 1994, Intercalibration of astronomical and radioisotopic time: Geology, v. 22, p. 783–786

Retallack, G.J., 1983, Late Eocene and Oligocene paleosols from Badlands National Park, South Dakota: Geological Society of America Special Paper 193, 82 p.

Retallack, G.J., 1992, Paleosols and changes in climate and vegetation across the Eocene-Oligocene boundary, *in* Prothero, D.R., and Berggren, W.A., eds., Eocene-Oligocene climatic and biotic evolution: Princeton, Princeton University Press, p. 383–398.

Retallack, G.J., 1994, The environmental factor approach to the interpretation of paleosols, *in* Amundson, R., Harden, J., and Singer, M., eds., Factors of soil formation: A fiftieth anniversary retrospective: Madison, Wisconsin, Soil Science Society of America Special Publication 33, p. 31–64.

Retallack, G.J., 1997a, Neogene expansion of the North American prairie: Palaios, v. 12, p. 380–390.

Retallack, G.J., 1997b, Early forest soils and their role in Devonian global change: Science, v. 276, p. 583–585.

Retallack, G.J., 2000, Depth to pedogenic carbonate horizon as a paleoprecipitation indicator: Comment: Geology, v. 28, p. 572–573.

Retallack, G.J., 2001a, Cenozoic evolution of grasslands and climatic cooling: Journal of Geology, v. 109, p. 407–426.

Retallack, G.J., 2001b, A 300-million record of atmospheric carbon dioxide from fossil plant cuticles: Nature, v. 411, p. 287–290.

Retallack, G.J., 2002, Carbon dioxide and climate over the past 300 Myr: Royal Society of London Philosophical Transactions, v. A360, p. 659–673.

Retallack, G.J., Bestland, E.A., and Fremd, T.J., 2000, Eocene and Oligocene paleosols of central Oregon: Geological Society of America Special Paper 344, 192 p.

Richardson, H.E., 1950, The geology of the Sweet Home fossil forest [M.S. thesis]: Eugene, University of Oregon, 44 p.

Ridgway, K.O., Sweet, A.R., and Cameron, A.R., 1995, Climatically induced floral change across the Eocene-Oligocene transition in the northern high latitudes, Yukon Territories, Canada: Geological Society of America Bulletin, v. 107, p. 676–696.

Robinson, P.T., Brem, G.F., and McKee, E.H., 1984, John Day Formation of Oregon: A distal record of early Cascade volcanism: Geology, v. 12, p. 229–232.

Rouse, G.E., and Matthews, W.H., 1979, Tertiary geology and paleontology of the Quesnel area, British Columbia: Bulletin of Canadian Petroleum Geology, v. 27, p. 418–445.

Royer, D.L., 1999, Depth to pedogenic carbonate horizon as a paleoprecipitation indicator?: Geology, v. 27, p. 1123–1126.

Sanborn, E.L., 1935, The Comstock flora of west central Oregon: Carnegie Institution of Washington Publication 465, p. 1–28.

Sanborn, E.L., 1949, The Scio flora of west central Oregon: Studies in Geology, Oregon State University, v. 4, p. 1–47.

Schenk, H.G., 1923, A preliminary report of the geology of the Eugene Quadrangle, Lane and Linn Counties, Oregon [M.S. thesis]: Eugene, University of Oregon, 104 p.

Schenk, H.G., 1936, Nuculid bivalves of the genus *Acila*: Geological Society of America Special Paper 4, 149 p.

Scholl, D.W., Stevenson, A.J., Noble, M.A., and Rea, D.R., 2003, The Meiji Drift body and Late Paleogene-Neogene paleoceanography of the North Pacific and Bering Sea region, *in* Prothero, D.R., Ivany, L.C., and Nesbitt, E., eds., From Greenhouse to Icehouse: The Marine Eocene-Oligocene Transition: New York, Columbia University Press, p. 119–153.

Schweitzer, C.E., and Feldman, R.M., 2000, New fossil portunids from Washington, USA and Argentina, and a re-evaluation of generic and family relationships within the *Portunoidea Rafinesque* 1815 (Decapoda, Brachyura): Journal of Paleontology, v. 74, p. 636–652.

Sheldon, N.D., and Retallack, G.J., 2001, Equation for compaction of paleosols during burial: Geology, v. 29, p. 247–250.

Sheldon, N.D., Retallack, G.J., and Tanaka, S., 2002, Geochemical climofunctions from North American soils and application to paleosols across the Eocene-Oligocene boundary in Oregon: Journal of Geology, v. 110, p. 682–696.

Sherrod, D.R., and Smith, J.G., 2000, Geologic map of Eocene to Holocene volcanic and related rocks of the Cascade Range, Oregon: U.S. Geological Survey Miscellaneous Investigations 110, 14 p.

Shroba, C.S., 1992, Paleoecology and taphonomy of middle Tertiary and recent sediments from Oregon and Washington, and biogeographic affinities of the Wallowa terrane, eastern Oregon [Ph.D. thesis]: Eugene, University of Oregon, 181 p.

Smith, J.G., Sawlan, M.S., and Katcher, A.C., 1980, An important lower Oligocene welded-tuff marker bed in the western Cascade Range of southern Oregon: Geological Society of America Abstracts, v. 12, p. 153.

Smith, G.A., Manchester, S.R., Ashwill, M., McIntosh, W.C., and Conrey, R.M., 1998, Late Eocene-early Oligocene tectonism, volcanism and floristic change near Gray Butte, central Oregon: Geological Society of America Bulletin, v. 110, p. 759–778.

Smith, W.D., 1938, The geology and mineral resources of Lane County, Oregon: Oregon Department of Geology and Mineral Industries Bulletin, v. 11, 65 p.

Smith-Gharet, L.R., 1999, Oligocene fossils of Salem: Rock and Gem, v. 9, p. 68–70.

Spicer, R.A., and Wolfe, J.A., 1987, Plant taphonomy of the late Holocene deposits in Trinity (Clair Engle) Lake, northern California: Paleobiology, v. 13, p. 227–245.

Squires, R.C., 2003, Turnovers in marine gastropod faunas during the Eocene-Oligocene transition, west coast of the United States, *in* Prothero, D.R., Ivany, L.C., and Nesbitt, E., eds., From Greenhouse to Icehouse: The Marine Eocene-Oligocene Transition: New York, Columbia University Press, p. 14–35.

Staples, L.W., 1950, Cubic pseudomorphs of quartz after halite in petrified wood, Oregon: American Journal of Science, v. 248, p. 124–136.

Staples, L.W., 1965, Zeolite filling and replacement in fossils: American Mineralogists, v. 50, p. 1796–1801.

Steere, M.J., 1958, Fossil localities of the Eugene area, Oregon: The Ore Bin, v. 20, p. 51–59.

Strömberg, C.A.E., 2002, The origin and spread of grass-dominated ecosystems in the late Tertiary of North America: Preliminary results concerning the evolution of hypsodonty: Palaeogeography, Palaeoclimatology, Palaeoecology, v. 177, p. 59–75.

Swisher, C.C., and Prothero, D.R., 1990, Single crystal $^{40}Ar/^{39}Ar$ dating of the Eocene-Oligocene transition in North America: Science, v. 249, p. 760–762.

Tanai, T., and Wolfe, J.A., 1977, Revisions of *Ulmus* and *Zelkova* in the middle and late Tertiary of western North America: U.S. Geological Survey Professional Paper 1026, 14 p.

Torley, R.F., and Hladky, F.R., 1999, Silicic volcanism in the Cascade Range; evidence from Bear Creek and Antelope Creek valleys, southern Oregon: Oregon Geology, v. 61, p. 122–123.

Turner, S., Hawksworth, C., Liu, J., Rogers, N., Kelley, S., and van Calsteren, P., 1993, Timing of Tibetan uplift by analysis of volcanic rocks: Nature, v. 364, p. 50–54.

van Frank, R., 1955, *Palaeotaricha oligocenica*, new genus and species; an Oligocene salamander from Oregon: Breviora, v. 45, p. 1–12.

Vokes, H.E., and Snavely, P.D., 1948, The age and relationships of the Eugene and Fisher Formations: Geological Society of Oregon Country Newsletter, v. 14, no. 5, p. 39–41.

Vokes, H.E., Snavely, P.D., and Myers, D.A., 1951, Geology of the southern and southwestern border areas, Willamette Valley, Oregon: U.S. Geological Survey Oil and Gas Investigation Map OM110, scale 1:63,360, 1 sheet.

Vonhof, H.B., Smit, J., Brinkhuis, H., Montanari, A., and Nederbragt, A.J., 2000, Global cooling accelerated by early late Eocene impacts?: Geology, v. 28, p. 687–690.

Washburne, C.W., 1914, Reconnaissance of the geology and oil prospects of northwestern Oregon: U.S. Geological Survey Bulletin, v. 590, 111 p.

Weaver, C.E., 1942, Paleontology of the marine Tertiary formations of Oregon and Washington: University of Washington Publications in Geology, v. 5, 790 p.

Wells, R.E., 1990, Paleomagnetic rotations and the Cenozoic tectonics of the Cascade Arc, Washington, Oregon, and California: Journal of Geophysical Research, v. 95, p. 19,409–19,417.

Welton, B.J., 1972, Fossil sharks in Oregon: The Ore Bin, v. 36, p. 161–170.

Wilson, H., and Treasher, R.C., 1938, Preliminary report of some refractory clays of western Oregon: Department of Geology and Mineral Industries Oregon Bulletin, v. 6, 93 p.

Wolfe, J.A., 1968, Paleogene biostratigraphy of non-marine rocks in King County, Washington: U.S. Geological Survey Professional Paper 571, 33 p.

Wolfe, J.A., 1971, Tertiary climate fluctuations and methods of analysis of Tertiary floras: Palaeogeography, Palaeoclimatology, Palaeoecology, v. 9, p. 27–57.

Wolfe, J.A., 1977, Paleogene floras from the Gulf of Alaska region: U.S. Geological Survey Professional Paper 997, 108 p.

Wolfe, J.A., 1978, A paleobotanical interpretation of Tertiary climate in the Northern Hemisphere: American Scientist, v. 66, p. 694–703.

Wolfe, J.A., 1981a, Paleoclimatic significance of the Oligocene and Neogene floras of the northwestern United States, *in* Niklas, K.J., ed., Paleobotany, paleoecology and evolution: New York, Praeger, p. 79–101.

Wolfe, J.A., 1981b, A chronologic framework for Cenozoic megafossil floras of northwestern North America and its relation to marine geochronology, *in* Armentrout, J.M., ed., Pacific Northwest biostratigraphy: Geological Society of America Special Paper 184, p. 39–47.

Wolfe, J.A., 1992, Climatic, floristic and vegetational changes over the Eocene/Oligocene boundary in North America, *in* Prothero, D.R., and Berggren, W.A., eds., Eocene-Oligocene climatic and biotic evolution: Princeton, Princeton University Press, p. 421–436.

Wolfe, J.A., 1993, A method of obtaining climatic parameters from leaf assemblages: U.S. Geological Survey Bulletin, v. 2040, 71 p.

Wolfe, J.A., 1994, Tertiary climatic changes at middle latitudes of western North America: Palaeogeography, Palaeoclimatology, Palaeoecology, v. 108, p. 195–205.

Wolfe, J.A., 1995, Paleoclimatic estimates from Tertiary leaf assemblages: Annual Reviews of Earth and Planetary Sciences, v. 24, p. 119–142.

Wolfe, J.A., and Spicer, R.A., 1999, Fossil leaf character states: Multivariate analyses, *in* Jones, T.P., and Rowe, N.P., eds., Fossil plants and spores: Modern techniques: London, Geological Society, p. 233–239.

Wolfe, J.A., and Tanai, T., 1987, Systematics, phylogeny and distribution of *Acer* (maples) in the Cenozoic of western North America: Journal of the Faculty of Science Hokkaido University, v. 22, p. 1–246.

Wolfe, J.A., Forest, C.E., and Molnar, P., 1998, Paleobotanical evidence of Eocene and Oligocene paleoaltitudes in mid-latitudinal western North America: Geological Society of America Bulletin, v. 110, p. 664–678.

Woller, N.M., and Priest, G.F., 1982, Geology of the Lookout Point area, Lane County, Oregon: Open-file Report Oregon Department of Geology and Mineral Industries, v. O-82-7, p. 119–134.

Zachos, J., Pagani, M., Sloan, L., Thomas, E., and Billups, K., 2001, Trends, rhythms and aberrations in global climate 65 Ma to present: Science, v. 292, p. 689–693.

Manuscript Received by the Society 22 October 2002
Revised Manuscript Received 5 June 2003
Manuscript Accepted 14 August 2003

Printed in the USA